CHAPTER II

SECTION – I

A di - μ – oxomolybdenum(V) complex of 6-acetonyl-isoxanthopterin, undergoing oxygen atom transfer with dimethyl sulphoxide.

Abstract

The new compound, $Na[(Mo^{V}_2O_4)(pte_l)(OCH_3)(CH_3OH)_2]$ (pte_l = anion of 6-acetonyl-isoxanthopterin), has been prepared using the redox 'non-innocent' title ligand in $CH_3OH - H_2O$, and characterized by elemental analysis and physico-chemical methods including, ESIMS, IR, UV-VIS, ^{1}H-NMR spectra and CHEM3D representations. Rate constant data for its oxygen atom transfer (OAT) reaction with dimethyl sulphoxide (DMSO) tally with those of synthetic analogue systems reported earlier by different authors. The negative activation entropy ($\Delta S^{\#} = -206.3$ J mol $^{-1}$ deg $^{-1}$) is consistent with an associative mechanism for this reaction.

LIBRARY
NBU DARJEELING

216462

02 DEC 2003

Introduction

Pterin derivatives, specially those with different types of 6-substituent, have been found in many matalloenzymes, where the metal atom may be Mo for molybdoenzymes, W for tungstopterin enzymes, and Fe or Cu for aromatic amino acid hydroxylases [1,2, 81, 82] . The well-known ability of the pterin ring to act as a redox partner in biological redox systems, is intimately connected with the ability of the pyrazine moiety (pterin ring) to exist in different oxidation states [4]. These facts have inspired symbiotic developments in the coordination Chemistry of pterin ligands [3(a,b), 20]. In view of the multi-electron redox capability of both the molybdenum atom (VI, V, IV) and the pterin ligand, the redox aspect of molybdenum – pterin interaction and the reactivity of the resulting compounds still need careful study [3(a,b)].

This work is connected with the synthesis, characterization and reactivity study towards DMSO, of a new di-nuclear molybdenum (V) complex of 6-acetonyl-isoxanthopterin [$H_2(pte_I)$, Scheme (II – 1)], whose 7-oxo group corresponds to the pyran ring oxygen atom of Mo-centered Functional Unit (McFU) [1, 2] [Scheme (I–1)]. As delineated here, $H_2(pte_I)$ acts as a reducing agent towards Na_2MoO_4 in a $CH_3OH - H_2O$ medium during the synthesis of the above mentioned complex.

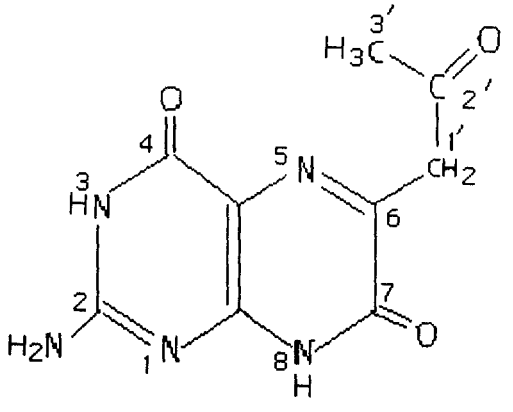

Scheme (II - 1)

Experimental

Materials: Reagent grade chemicals were used as received. Solvents were purified, prior to use, following literature procedure [9]. $Na_2MoO_4\ 2H_2O$ was obtained from BDH, E. Merck, Mumbai. Et_4NBr was obtained from Fluka Chemica. Kinetic and electrochemical measurements were performed in spectroscopic grade DMSO (SRL, Mumbai). Bu_4NClO_4 (TBAP) for CV measurements, was obtained by published methods [11].

Method: Elemental analysis (C,H,N) data were obtained from the IACS, Kolkata. Molybdenum was estimated by atomic absorption spectroscopy. ^{1}H-NMR data in DMSO-d_6 were obtained from the IISc, Bangalore (Bruker, DRX 500 MHz), RSIC, Lucknow (Bruker, DRX 300 MHz) and TIFR, Mumbai (Bruker, AMX 500 MHz). The electrospray mass spectra in CH_3OH were obtained from RSIC, Lucknow (Micromass Quattro II triple quadrupole mass spectrometer). IR spectra (nujol mull) were recorded on a Philip Analytical SP3 – 300 spectrometer. Electrical conductivity data in DMF and DMSO (0.8 mmol dm^{-3} solution) were measured using a digital conductivity meter (Systronics, model 304). Cyclic voltammetry data (vs. SCE, uncorrected for the junction contribution) were recorded under a N_2- atmosphere on a BAS (CV–27), USA instrument. Electronic spectra and kinetic data (under N_2- atmosphere) were recorded on a Shimadzu (UV–240) spectrophotometer, with thermostatic conditions (± 0.5 K) being maintained using a Shimadzu (TB–85) thermostat. Pseudo-first-order rate constants (k_{obs}, s^{-1}) were determined by the least square method from the plots of $\log(A_\infty - A_t)$ vs. time, which were linear for at least three half-lives. These rate constants were used to determine activation parameters by means of an Eyring plot [$\ln (k_{obs}/T)$ vs. $(1/T)$]; relevant data are collected in Table (II – 4). Magnetic susceptibility measurement were done with a Gouy balance, using $Hg[Co(SCN)_4]$ as calibrant.

Synthesis of the complexes

6-acetonyl-isoxanthopterin, H_2pte_I. 0.5 H_2O (1)

The pterin ligand (**1**) was prepared in 75 % yield by modifying the original method of synthesis in the light of later developments (e.g., darkness, N_2 – atmosphere, pH = 6.8) [6]. Purity of the product was checked through TLC [silica-gel GF_{254}, UV – lamp], using CH_3OH – H_2O (4 : 1, v/v) solution and Me_2CO – Et_2O (1 : 1, v/v) as eluant. R_f : 0.65. The product gave positive 2,4 – DNP test and decomposed without melting above 573 K. Its solubility is ca. 5% in DMF (warming and stirring). Found : C, 44.0; H, 4.4; N, 28.4 %. Calc. for $C_9H_9N_5O_3.0.5\ H_2O$: C, 44.3; H, 4.1; N, 28.7 %. UV – VIS absorption bands [DMF, $\lambda_{max}^{nm}(\log\epsilon)$]: 293 (3.68), 341 (3.86), 400 (3.28), 422 (3.27), 456 sh (3.00).

$Na[(Mo^V_2O_4)(pte_I)(OCH_3)(CH_3OH)_2]$ (2)

A purged (N_2) aqueous solution (10 ml) of $Na_2MoO_4.2H_2O$ (0.242 g, 1 mmol) was treated with a stirred suspension of 6-acetonyl-isoxanthopterin hemihydrate (0.244 g, 1 mmol) in CH_3OH (100 ml) under N_2 in dark, pH adjusted to 4.8 (AcOH); finally a CH_3OH solution (10 ml) of Et_4NBr (0.525 g, 2.5 mmol) was added and stirring was continued for 25 h (301 K). The light yellow compound was recovered by filtration (fritte) under N_2 in dark, washed with purged solvents [e.g., CH_3OH – H_2O (1 : 1, v/v), CH_3OH, Et_2O], dried in vacuo over silica gel for 48 h. Yield : 60 %. Its purity was checked through TLC [silica-gel GF_{254}, UV–lamp], using diluted (with 50 times CH_3OH) DMSO solution and CH_2Cl_2 – benzene (1 : 1, v/v) as eluant. R_f : 0.54. Its solubility is ca. 4% in DMF. Found : C, 24.1; H, 3.1; N, 11.7; Mo, 31.9 %. Calc. for $NaMo_2O_{10}C_{12}H_{18}N_5$: C, 23.7; H, 3.0; N, 11.5; Mo, 31.6 %. UV-VIS absorption bands [DMF, $\lambda_{max}^{nm}(\log\epsilon)$]: 291 (4.03), 342 (4.25), 400 (3.56), 422 sh (3.53), 458 sh (3.23) [1,2]. The compound is found to be diamagnetic in nature.

Results and Discussion

The ligand (**1**) [Scheme (II–1)] used in this work is a 6 – substituted pterin compound and the reason behind its choice is to explore its participation in the redox activity at the Mo centre of the pertinent molybdenum complex (**2**) [Fig.(II–9a)] [4, 119]. Low solubility associated with hydrogen bonding (involving hydrophilic group like amino, hydroxo, etc.) is a characteristic feature of pterin Chemistry [84(b)]. But there is a good agreement between the experimental analytical data and the expected values for (**1**) and (**2**).

Electrospray Ionization Mass Spectroscopy (ESIMS) involving soft ionization technique, has proved to be a valuable tool for characterizing wide variety of compounds including inorganic and coordination sphere [12, 110, 121]. This technique helps in assigning the molecular mass of this type of synthetic compounds[12, 85, 107] . As true for different types of mass spectrometry, the assignment of molecular formula (or any definite fragment originating from it) is confirmed by the experimental value of m/z (most abundant isotopic mass) as well as matching between the experimental and calculated (simulated) isotopic distribution profile [14, 85, 107, 117, 118]. As far as organic compounds containing O, F, P and I are concerned, the relative intensities of M, M+1 and M+2 isotope peaks are of great value in recognizing the molecular ion (M^+) peak or any well – defined fragment containing it [85]. For (**1**), the ESIMS spectrum contains its molecular ion peak without $0.5H_2O$, at m/z = 235.9 (relative abundance = 63 %). All the other fragmentation and fragment association peaks are also assigned as per the proposed molecular formula. In case of (**2**), the molecular ion peak appeared at m/z = 609.1, $[M + 2H]^+$ (relative abundance = 38.1 %), where 'M' corresponds to the molecular formula of (**2**)[85, 107] ; it is associated with the characteristic distribution of molybdenum isotopes [7(a), 14, 15]. The ligand $[H_2pte_1]^+$ peak is observed at m/z = 235.9 (relative abundance = 89.2 %). Breaking up of (**2**) to some extent during recording of ESIMS data along with cluster formation (m/z = 825.0, relative abundance = 16.2 %) is indicated [12(a)].

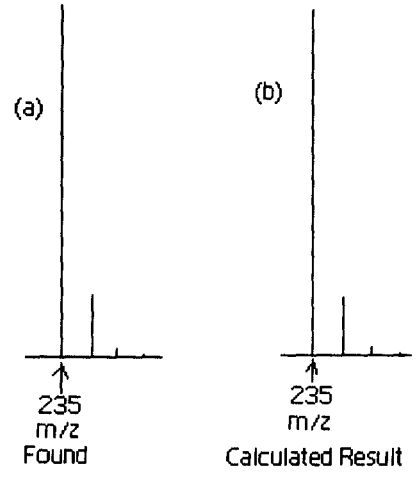

Fig.(II–1): (a) ESIMS data of (**1**) at m/z (= 235) region corresponding to $[H_2pte_1]^+$; (b) the calculated isotope pattern [46]. Formula: $C_9H_9N_5O_3$.

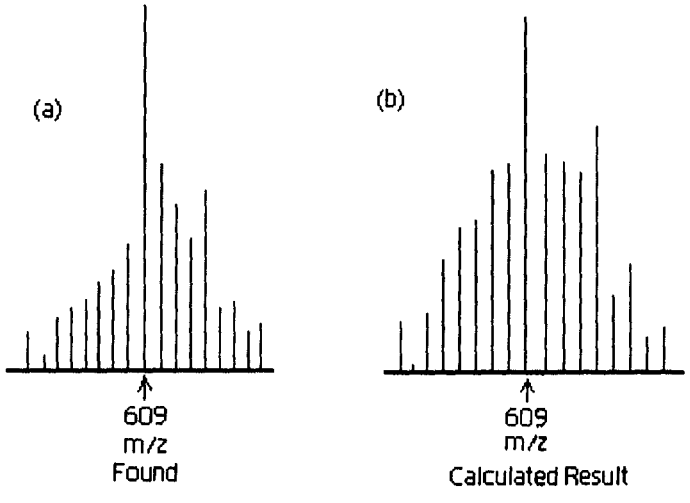

Fig.(II–2): (a) ESIMS data of (**2**) at m/z (= 609) region corresponding to $[M + 2H]^+$; (b) the calculated isotope pattern [46]. Formula: $C_{12}H_{20}N_5O_{10}Mo_2Na$.

The molecular ion peak of (**1**) at m/z = 235 and that of (**2**) at m/z = 609.1, mentioned above, is simulated with the help of a computer program, 'Isotope Pattern Calculator' (IPC) [46] and found to be in good agreement with the experimentally obtained data [Fig.s(II–1) & (I–1) respectively] suggesting the accuracy of molecular mass prediction of these compounds.

The Λ_M values of (**2**) (ohm $^{-1}$cm ^{2} mol $^{-1}$, 301 K) = 27 (DMSO) and 73 (DMF) are consistent with its 1 : 1 electrolytic formulation [13].

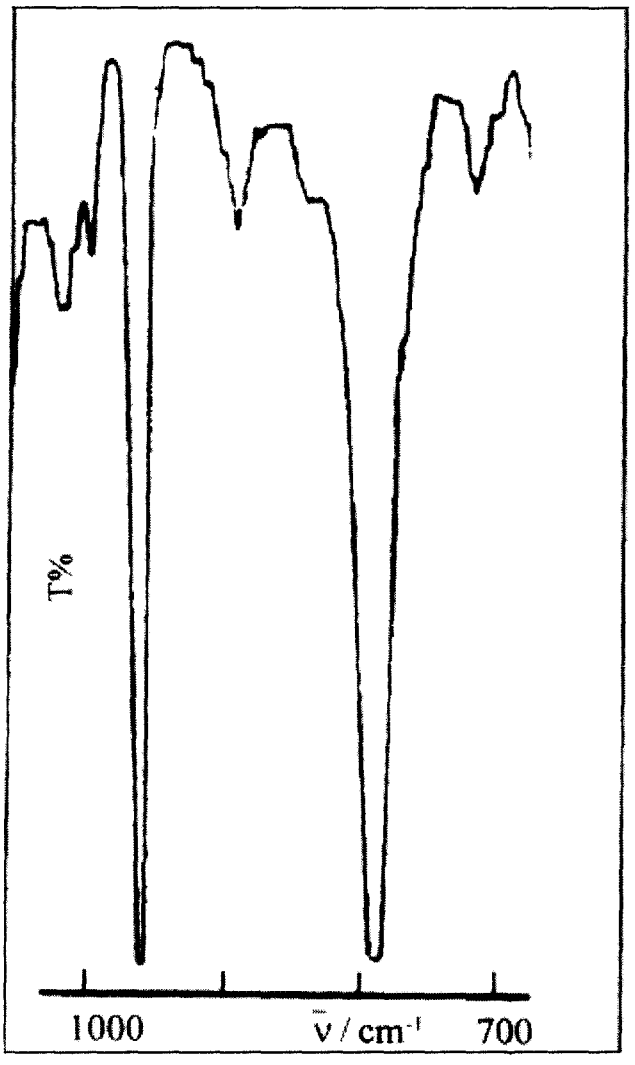

Fig.(II – 3): IR spectrum (nujol) of (**2**).

Comparison of the IR spectra of (**1** & **2**), shows that the three ligand bands in the 1600 – 1700 cm $^{-1}$ region undergo considerable modification due to deprotonation of NH(3) and NH(8) groups [Scheme (II–1)] through enolisation involving the 4 – and 7 – oxo groups respectively, followed by coordination through O(4) and N(5) atoms[3(a,b), 20(a,d), 27] [Fig.(II–9a)]. For (**2**) the ν(C=O) mode of the 2′ - oxo group appears as a strong band at 1645 cm^{-1}; the ν(C=C), ν(C=N) vibrations of the pterin ring are associated with this band[5, 6, 15, 16, 48]. The characteristic IR bands of the $(Mo^{V}_{2}O_{4})^{2+}$ core in (**2**) appear at their expected positions [Fig.(II–3)]; as (**2**) has been obtained from a CH_3OH – H_2O reaction medium (pH = 4.5), presence of a di-μ-oxo core is quite likely[29].

In C_{4v} symmetry the d orbitals transform according to a_1 (d_{z^2}), b_1 ($d_{x^2-y^2}$), b_2 (d_{xy}) and e (d_{xz}, d_{yz}) representations, and the d – orbital (ligand field) portion of the MO diagram is shown in Fig.(II–4). The a_1 level is strongly sigma anti-bonding due to interaction with a pσ orbital on O atom and (a weaker interaction) with a pσ orbital on the trans group. The d_{xz} and d_{yz} orbitals are involved in strong pi bonding with O p_x and p_y orbitals and as a result the e level is significantly raised in energy above the b_2 (d_{xy}) level.

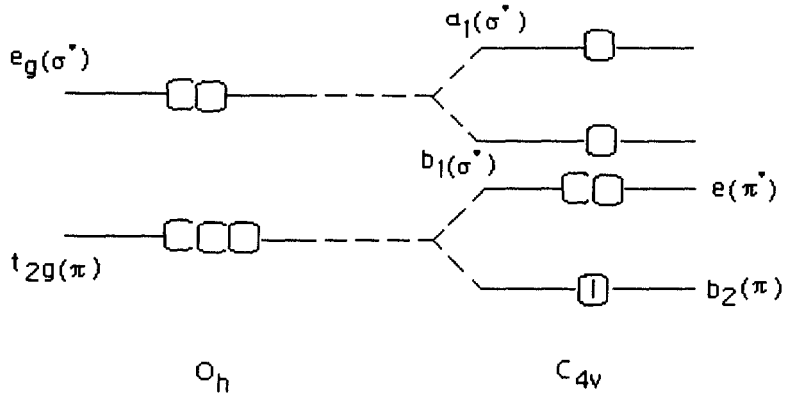

Fig.(II – 4): Ligand – field splitting Diagram for C_{4v} complexes.

The distorted octahedral geometry of (**2**) [as bond angles data in Table(II–3)] leads to further ligand field splitting of d – orbitals (as compared to the usual e_g and t_{2g} level of O_h symmetry) and favours spin pairing in the d_{xy} (b_2) level[19]. Of the three chemically relevant oxidation states of molybdenum (e.g., Mo^{IV}, Mo^{V} and Mo^{VI}), during catalysis only the Mo^{V} (d^1) state could be detected as a transient species by EPR spectroscopy in oxomolybdoenzymes ; the Mo^{IV} (d^2) state is consistently diamagnetic in such cases [26]. Almost all the synthetic molybdenum pterin complexes reported so far are diamagnetic, including one formulated as containing a Mo^{V} centre; diamagnetic behaviour of the latter system is explained by invoking a strong antiferromagnetic coupling between the d^1 (Mo^{V}) electron and the delocalized electron system of the redox "noninnocent" pterin ligand [20(a,d)]. This unique nature of the pterin ligand is responsible for the observed diamagnetism of (**2**) and its high resolution ^1H NMR data. The diamagnetic nature of (**2**) is also consistent with the observations on well – characterized dinuclear μ – oxomolybdenum (V) complexes where the spins of the two d^1 centres are antiferromagnetically coupled involving the 2p orbital of the bridging oxygen atom [19].

For **(1)** [Table (II – 1)] ^{1}H-NMR signals of the $CH_3(3')$ and $CH_2(1')$ groups [Scheme (II – 1)] appear as singlets at δ, 2.18 and δ, 3.74 respectively; these spectral assignments have been carried out on the basis of ^{1}H-^{1}H COSY data [Fig.(II–6)], supported by proton integration values. In view of the oxo-transfer reaction of **(2)** with DMSO, several of its high resolution ^{1}H-NMR spectra were recorded for unambiguous spectral assignments. One such spectrum [Fig.(II–5)] shows the $CH_3(3')$ and $CH_2(1')$ signals at δ, 1.16 and δ, 3.21 respectively. ^{1}H-^{1}H COSY data (500 MHz, 280 K) help to identify the $CH_3(3')$ (δ 1.18, triplet, J = 7.5 Hz) and $CH_2(1')$ (δ 3.22, quartet, J = 7.7 Hz) signals; the J – values were estimated from the corresponding 2D – J resolved spectrum [Fig.(II–7)]. In Fig.(II–5) the CH_3 signal of the two CH_3OH molecules and CH_3O – group appear together with the residual proton signal (H_2O) at δ, 3.38.

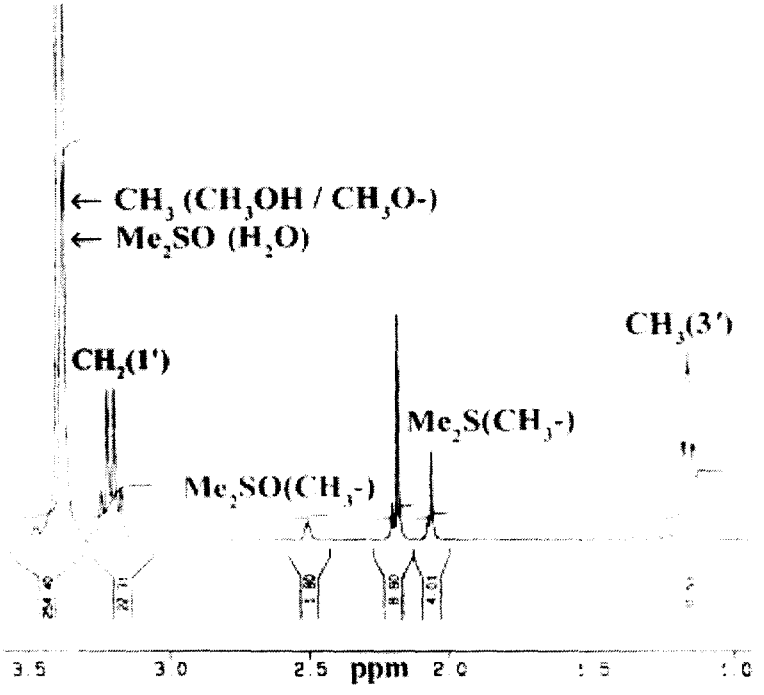

Fig.(II–5):300 MHz (298 K) ^{1}H NMR spectrum in DMSO – d_6 (δ, ppm vs. TMS) of **(2).**

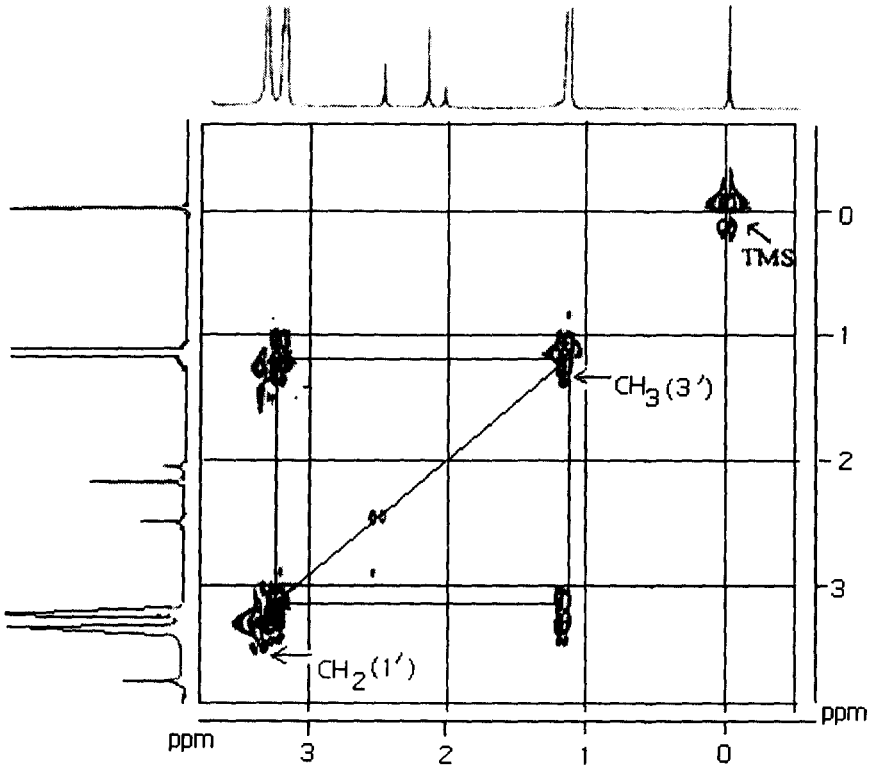

Fig. (II– 6) : 500 MHz (280 K) $^1H - ^1H$ COSY data of (**2**) in DMSO – d_6.

Table (II – 1): Relevant ^1H-NMR signals in DMSO – d_6 (δ ppm, internal TMS) of (**1**) & (**2**), and Δ (= $\delta_{compound}$ - δ_{ligand}) values.

Compound [a]	$CH_3(3')$	$CH_2(1')$
(**1**)[b]	2.18 (s)	3.74 (s)
(**2**)[c]	1.16 (t)	3.21 (q)
Δ	– 1.02	– 0.53

[a] Vide Scheme (II – 1) for proton numbering system; [b] data at 500 MHz, 300 K; [c] data at 300 MHz, 298 K.

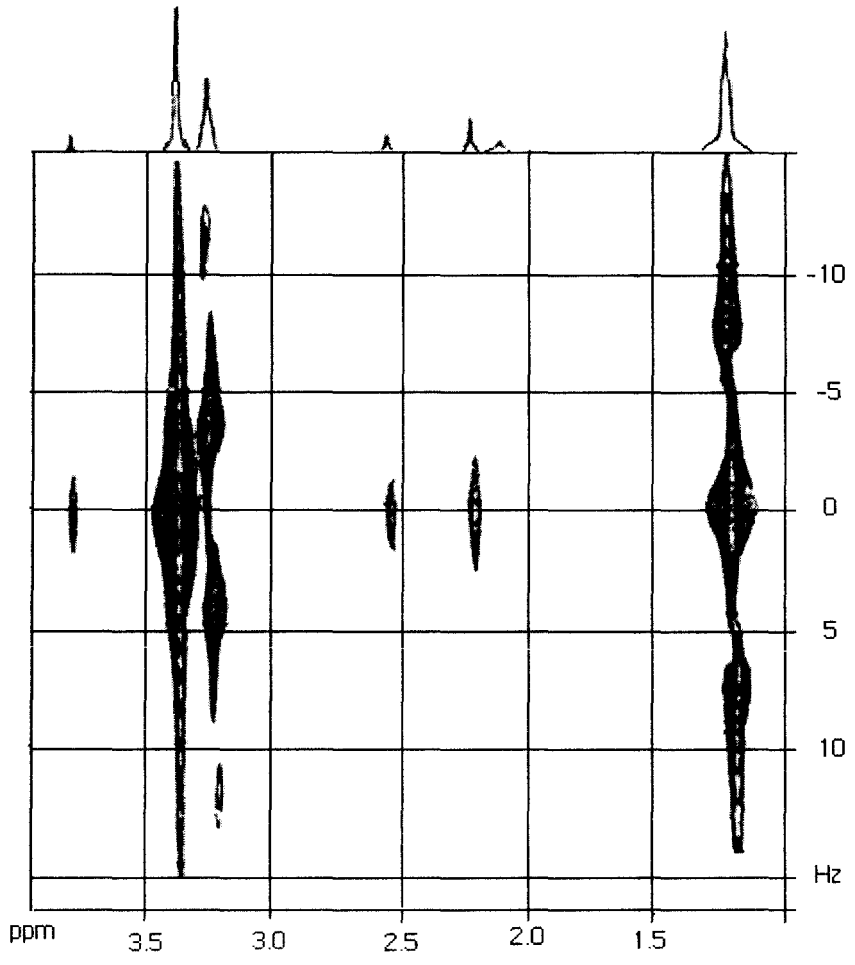

Fig. (II–7) : 500 MHz (280 K) 2D J resolved spectrum in DMSO – d_6 of (**2**).

For (**2**), the – NH_2 (2) signal (500 MHz, 280 K) consists of a broad prominent signal at δ 7.0, associated with two weaker ones at δ 6.75 and 6.50 due to the two additional forms = N^+H_2 and =NH [Fig.(II–9c) & (II–9a)] respectively. The proton integration data for the two protons of the – NH_2 (2) group (involving the three above – mentioned signals) tally with those of the two – OH signals of the two CH_3OH molecules in (**2**). As suggested by different authors, such transformations involving the – NH_2 (2) group are quite likely and help the pterin ring to play an active part essential for enzyme reactions [3(a,b), 5, 35]. Although the – OH signal of CH_3OH (neat) usually appears at ca. δ 5.0, in (**2**), the two CH_3OH molecules exhibit two separate – OH signals [due to the overall unsymmetrical nature of (**2**), Fig.(II–9a)] at δ, 12.35 and δ 10.96. Depletion of

electron density associated with strong coordination to the Mo^{V} – atoms [29], is responsible for the substantial deshielding of these – OH signals of CH_3OH in (**2**). Coordination of the CH_3OH molecule to the molybdenum atom in different types of compound, sometimes leading to deprotonation / methoxide coordination, has been proposed by various workers and has been characterized by X-ray crystallographic data [3(a,b), 20(a,d), 18, 27]. The electronic effects associated with the possible existence of the – NH_2 (2) group in two additional forms [Fig.(II–9a) & (II–9c)] as stated above, are transmitted (via the pterin ring) even upto the two coordinated CH_3OH molecules in (**2**); this is evident from the fact that each major methanolic – OH signal is accompanied by two minor ones. A comparative study [Table (II–1)] of the splitting patterns of the $CH_3(3')$ and $CH_2(1')$ signals in (**1**) and (**2**) also throws light on the above-mentioned electronic circulation effect. In (**1**), these two signals appear as singlets, whereas in (**2**) they are split up into a triplet and a quartet respectively. Although ^{1}H-^{1}H COSY data indicate spin – spin interaction between these two signals in both these cases, most likely the increased electronic circulation due to coordination in (**2**) is responsible for the observed splitting of the $CH_3(3')$ and $CH_2(1')$ signals in this case. Besides this, contrary to expectation the proton signals [Table (II - 1)] of (**2**) exhibit varying degree of shielding effects (negative Δ values) [83]. The +2 charge on the $(Mo^{V}_2O_4)^{2+}$ core is satisfied by the deprotonated O(4) atom and methoxide group; the additional electron density released through deprotonation of – NH(8) [Na^+ salt formation with O(7), consistent with Λ_M values] is transmitted via the redox 'non-innocent' pterin ligand to the region around the O(2′) atom of the 6-substituent [Scheme (II–1) & Fig.(II–9a) to (II–9c)], causing the observed shielding effect [3(a,b), 4, 20(a,d), 27]. This extra electron density around the $(Mo^{V}_2O_4)^{2+}$ core in (**2**), makes it a good reducing agent towards a typical enzyme substrate like DMSO, as revealed by following kinetic data; this process also indicates oxidation state less than VI for the Mo – atoms in (**2**). The proposed CHEM3D Representations of (**2**) involving a bridging pterin ligand is consistent with different types of structurally characterized bi-nuclear molybdenum (V) complexes including triply bridged ones as well as structurally characterized metal – pterin complexes where the N(5) atom (pterin residue) [Scheme (II–1)] plays a pivotal role [3(a,b), 5, 20(a,d), 29, 27, 39].

From the considerations of elemental analysis and ESIMS data (experimental and simulated) as well as other physicochemical data, the chemical compositions of the new compounds (ligand, complex and recovered complex) were established. Then their possible schematic structures were optimized by molecular mechanics calculations (MM2), giving the lowest steric energy [for (**1**) – 2.52 Kcal mol^{-1} and for (**2**) 13.95 Kcal mol^{-1}] CHEM3D model [e.g., Fig.(II–8) and Fig.(II–9a)], thereby throwing light on both stability and geometry of these compounds [87]. The molecular modelling force fields in use for molecular systems can be interpreted in terms of the four key contributions, e.g., bond stretching, angle bending, torsional terms and non-bonded interactions [86]; apart from the lowest steric energies of the molecules. Here, two basic parameters were evaluated, e.g., bond distances (Å) and bond angles (deg.). The most relevant of which are shown in Table (II–2) and Table (II–3), together with the available literature data on X–ray structural studies in the relevant fields [3, 5, 20(a-c), 27, 29, 114 - 116] and the data are in conformity with the recent trends of structure elucidation using optimized computational models [108].

Concentrating on the chelating aspect of the pterin ligand towards molybdenum, the Mo-N(5) bond plays a pivotal role here [atom numbering as per Scheme (II–1)] and this bond distance shows a fair agreement between the computed and experimental data [3, 5, 20(a-c), 27, 29, 114 – 116] [Table (II–2)].

The most stable CHEM3D representation for (**1**) [Fig.(II-8)] shows nothing but the same structure as proposed in Scheme (II–1) above. In case of (**2**), the most stable form [Fig.(II-9a)] (Steric energy = 13.95 Kcal mol^{-1}) shows the participation of N(12) lone pairs towards the formation of π – bond with the adjacent C(5) atom having neutral N(12) and N(6) atoms but retaining aromaticity in the pyrazine ring.

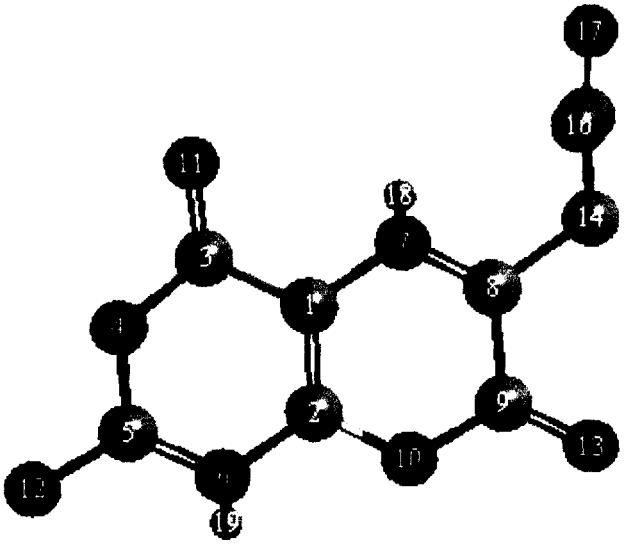

Fig. (II– 8): The optimized geometry (CHEM 3D model obtained through MM2 calculations) of (1) with a steric energy of – 2.52 Kcal mol^{-1}. Its numbering system is set by the software used[87] and is different from that in Scheme (II – 1).

Table (II – 2): Comparison of selected optimized bond lengths (Å) and bond angles (deg.) in the free ligand (1) and its molybdenum complex (2)

Atoms	Bond Distances(Å)$^+$	Atoms	Bond Distances(Å)$^+$
C(1)-N(7)	1.41 [1.40]	C(1)-C(3)	1.48 [1.44]
C(3)-O(11)	1.22 [1.36]	C(1)-C(2)	1.37 [1.41]
C(9)-O(13)	1.22 [1.36]	C(3)-N(4)	1.37 [1.32]
C(2)-N(6)	1.40 [1.41]	C(9)-N(10)	1.36 [1.37]
C(15)-C(16)	1.51 [1.51]	C(5)-N(12)	1.37 [1.31]
C(2)-N(10)	1.35 [1.36]	C(5)-N(6)	1.31 [1.45]
N(7)-C(8)	1.28 [1.33]	C(14)-C(15)	1.51 [1.52]
C(8)-C(9)	1.49 [1.48]	N(4)-C(5)	1.35 [1.44]
C(15)-O(17)	1.21 [1.22]	C(8)-C(14)	1.50 [1.51]

Angle Atoms	Bond Angle(deg.)[+]	Angle Atoms	Bond Angle(deg.)[+]
N(6)-C(5)-N(4)	120.9 [118.0]	C(1)-N(7)-C(8)	118.7 [103.6]
C(3)-N(4)-C(5)	124.8 [121.5]	C(1)-C(3)-N(4)	114.8 [121.4]
C(8)-C(9)-N(10)	114.9 [122.8]	N(6)-C(2)-C(1)	121.6 [121.0]
N(7)-C(8)-C(9)	123.0 [123.1]	N(10)-C(2)-C(1)	119.8 [118.9]
C(2)-N(10)-C(9)	122.7 [111.7]	N(7)-C(1)-C(2)	121.0 [129.1]
C(2)-N(6)-C(5)	119.7 [117.0]	C(3)-C(1)-C(2)	118.2 [118.6]

[+] Free ligand data are mentioned outside third bracket and the data derived from its molybdenum complex, (**2**), are mentioned within third bracket.

Comparing these two sets of data it is clear that both bond lengths and bond angles of the ligand residue have undergone a recognizable change in it's complex (**2**) suggesting definite complexation of the [H_2pte_1] ligand with molybdenum metal. In comparison to the free ligand (**1**), the following bond lengths are increased in the complex: C(3) – O(11) from 1.22Å to 1.36Å, N(7) – C(8) from 1.28 Å to 1.33Å and C(15) – O(17) from 1.21 Å to 1.22 Å. This observation is consistent with the O(11), N(7) and O(17) [Fig.(II–8)] atoms' bonding with the molybdenum atom [compare with Fig.(II–9a)] leading to depletion of electron density from the bonds immediate to the bonds between metal and these atoms (i.e., the bonds mentioned above) and hence the observed increase in bond lengths in the complex. The C(5) – N(12) bond length has undergone a decrease from (1.37 – 1.31)Å on complexation indicating the N(12) [N(2) as per Scheme – (II-1)] lone pairs' participation in metal coordination via the pterin rings [3(a,b), 5, 34, 35], as mentioned above. Some other bond lengths such as C(9) – O(13), C(1) – C(2), C(5) – N(6) etc. have also suffered visible change due to redistribution of overall electron density on metal coordination

In all the probable forms of (2) [Fig.(II–9a) to (II–9c)], one Na^+ ion is held by ionic force by the uni-negative O(13) atom. Another probable form containing N(12) – C(5) π bond, formed through the N(12) lone pairs' participation in this π bonding and acquiring positive and negative charges on N(12) and N(6) respectively [Fig.(II–9c)] found to be of moderately stable (Steric energy = 15.26 Kcal mol^{-1}).

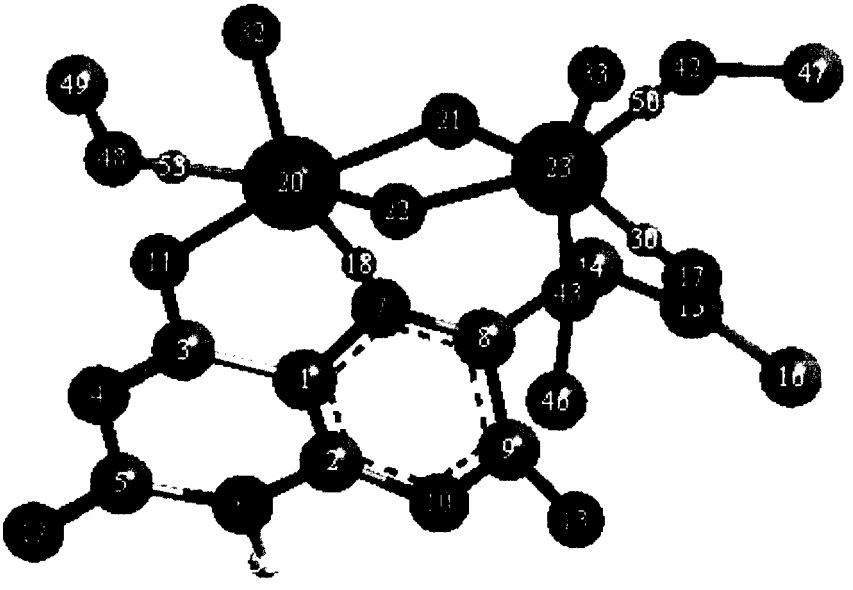

Fig.(II–9a): The optimized geometry (CHEM3D model obtained through MM2 calculations) of (2) with a steric energy of 13.95 Kcal mol^{-1}. Its numbering system is set by the software used[87] and is different from that in Scheme (II – 1).

Table (II–3): Comparison of selected computed bond lengths(Å) and bond angles (deg.) involving Mo – atom in (2) from the optimized geometry [Fig.(II–9a), MM2 calculations] with the available literature data (in parenthesis) from X-ray structural studies*

Atoms	Bond Distances(Å)$^+$	Atoms	Bond Distances(Å)$^+$
O(11)-Mo(20)	1.98(1.95–2.23)[3(c), 20a]	N(7)-Mo(20)	2.20(2.02)[3(c)]
O(42)-Mo(23)	2.14(2.32)[109]	Mo(20)-O(22)	1.97(1.93)[19]
O(21)-Mo(23)	1.97(1.93)[19]	O(48)-Mo(20)	2.24(2.32)[109]
Mo(23)-O(17)	2.18(2.01)[109]	Mo(23)-O(43)	1.97
Mo(20)-O(32)	1.98(1.66)[3(c)]	Mo(23)-O(33)	1.94(1.66)[108]

Angle Atoms	Bond Angle(deg.)$^{+}$	Angle Atoms	Bond Angle(deg.)$^{+}$
Mo(20)-N(7)-C(1)	120.8(119.3)[3(c)]	Mo(20)-O(11)-C(3)	119.1(112.1)[3(c)]
O(11)-Mo(20)-N(7)	80.6(74.1)[3(c)]	O(21)-Mo(23)-O(17)	109.0(105.9)[109]
Mo(20)-O(22)-Mo(23)	115.6	O(11)-Mo(20)-O(22)	137.9
O(33)-Mo(23)-O(22)	103.2	O(22)-Mo(20)-O(32)	90.3
O(21)-Mo(23)-O(22)	64.4	O(22)-Mo(20)-O(21)	64.0
O(17)-Mo(23)-O(33)	120.8	O(17)-Mo(23)-O(22)	125.3
Mo(20)-O(22)-Mo(23)	115.6	Mo(23)-O(21)-Mo(20)	114.9
O(22)-Mo(20)-N(7)	89.7	N(7)-Mo(20)-O(21)	72.3

$^{+}$ Here O(11), N(7) and O(17) correspond to O(4), N(5) and O(2′) donor atoms respectively, of the pterin ring as per Scheme (II – 1), while N(12) and N(6) correspond to the 2-substituent N and N(1) respectively.

* X-ray structural data have been collected from references mentioned as superscript on the data within parenthesis.

Table (II–3) shows few relevant bond length and bond angle data of (**2**), together with the X-ray structural data on molybdenum complexes of pterin ligand obtained from the available literature [3(c), 108, 109]. This approach of rationalizing optimized structural data, is in line with the recent trends in structure (and property) elucidation [48, 86, 108, 179]. The agreement between the computed bond lengths and the literature X-ray structural data is good, especially for O(11) – Mo(20) and N(7) – Mo(20), O(21)-Mo(23), O(48)-Mo(20) etc. [Table (II–3)]. Of the different donor atoms from the pterin ligand, the O(4) and N(5) atoms [this numbering system corresponds to Scheme (II–1)] play a major role in the metal-ligand bonding process which has been verified through X-ray crystallography [20(a,d), 27, 114 – 116]. From chemical and X-ray structural studies on 6-substituted pterins, it has been inferred that sufficiently greater basicity / nucleophilicity resides at N(5) than at N(8) of the pterin ring [Scheme (II–1)], thereby influencing its above-mentioned coordinating ability [88(a), 119]. Another important aspect is the close tally of Mo(23) – O(17) bond length from CHEM3D data with available X-ray data is noteworthy. Considering the length of 6 – substituted chain [numbering as per Scheme

(II–1)] of the ligand, the O(17) atom's coordination to the other molybdenum atom [Fig. (II–9a)] is possible and can be understood in the light of the peptide chain's coordination in oxomolybdoenzymes [2].

Table (II–2) shows the bond lengths and bond angles of the free ligand and that of the pterin ligand residue in the complex (2). Comparing these two sets of data it is clear that both bond lengths and bond angles of the pterin rings have undergone a visible change in it's complex suggesting definite complexation of the pterin ligand with molybdenum metal.

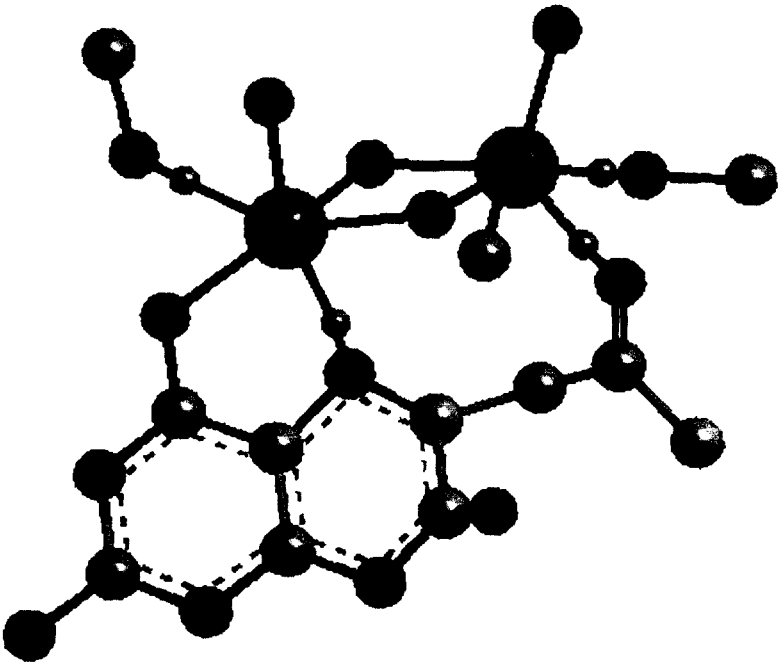

Fig.(II–9b):The optimized geometry (CHEM3D model obtained through MM2 calculations) of another tautomeric form of (2) with a steric energy of 65.54 Kcal mol^{-1}. Its numbering system is set by the software used[87] and is different from that in Scheme (II – 1).

The another form [Fig.(II–9b)] retaining aromaticity in both the pterin rings was found to be the least stable (Steric energy = 65.54 Kcal mol^{-1}). This form contains a single bond between N(12) and C(5). Here the planar nature of the aromatic rings hinders its stability in three dimensional space.

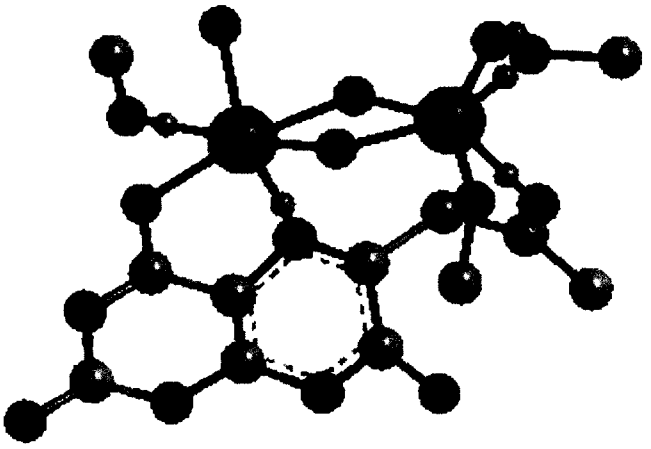

Fig.(II–9c): The optimized geometry (CHEM3D model obtained through MM2 calculations) of another tautomeric form of (**2**) with a steric energy of 15.26 Kcal mol^{-1}. Its numbering system is set by the software used[87] and is different from that in Scheme (II – 1).

In all the CHEM3D optimized geometries of three tautomeric forms of (**2**), presented above, contain an octahedral (slightly distorted) environment around both the molybdenum atoms, and the $(Mo^{V}_{2}O_{4})^{2+}$ core has cis disposition of its terminal oxygen atoms. That the $(Mo^{V}_{2}O_{4})^{2+}$ core is essentially in cis form is supported by the magnitude of O(33)-Mo(23)-O(22) and O(22)-Mo(20)-O(32) bond angles [Table(II–3)]. On the other hand, the trans form, which ought to be more stable in general, was found to possess higher amount of steric energy. This is due to the very nature of bonding in this molecule; here one side of the bridged oxo-molybdenum core is occupied by the bulky pterin ligand via its three coordination sites [Fig.(II–9a) to (II–9c)] leaving more space to the other side. So, the cis disposition of the terminal oxygen atoms provides less steric repulsion to the structure than the trans arrangement in this case.

Table(II–3) shows some important bond angles of (**2**) essentially belonging to four types of computed bond angles, in complete agreement with the four types of bond angles (62 ° – 77 °, 83 ° – 90°, 103 ° – 109 ° and 115 ° – 155 °) found from X-ray structural studies on different molybdenum – pterin systems with distorted octahedral geometry around the Mo – atoms (both mono and binuclear types)[3, 5, 20(a-c), 27, 114 – 116].

The above discussion on the geometrical aspect of optimized computational model (MM2) of a new complex compound, sharing agreement with available X-ray structural data (e.g., bond length, bond angle and overall geometry) verifies the applicability of such an approach to molybdenum – pterin systems and provides the frame work for discussion on their spectroscopic, reactivity and other relevant aspects [86, 108, 113].

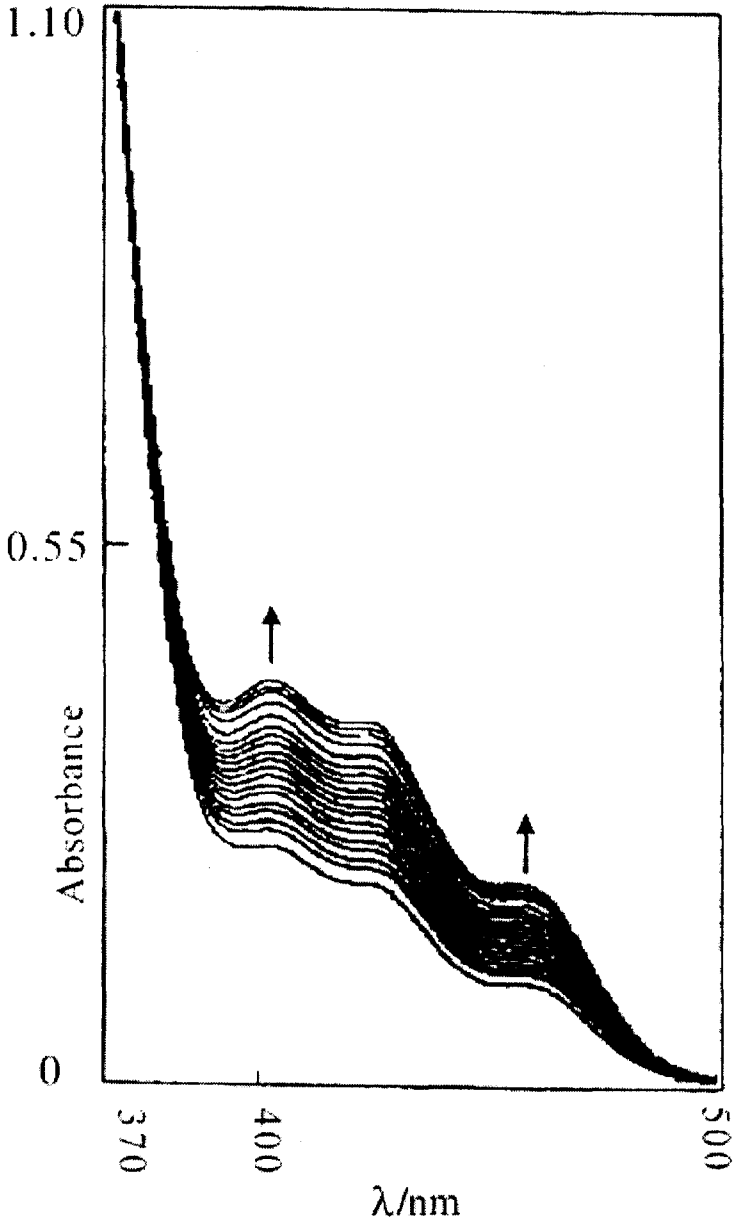

Fig.(II–10): UV – VIS absorption spectral changes recorded every 8 min. during the reaction of (**2**) [8.0×10^{-4}(M)] with DMSO at 299.5 K.

UV –VIS absorption bands of (**2**) contain all the pterin ligand's bands in (**1**) but in a slightly shifted position and with more intensity (higher logε values) (essentially $\pi \rightarrow \pi^*$ type), indicating more π – electron density in the ligand residue. This again can be explained by considering deprotonation from the pterin ligand during the complex formation reaction where the Mo^{VI} was reduced to Mo^{V} , and in this way pterin ligand acted as a reducing agent and subsequently itself got oxidized to more aromatic system [vide Fig.(II–8) to Fig.(II–9c)]. This argument is already substantiated by the NMR discussion and the kinetic studies discussed below.

The characteristic transitions of pterins in the 220 – 500 nm region depend to a large extent on the oxidation state and the tautomeric form of this ring system[3(a,b), 20(a,d), 23, 27]. The electronic spectral band of (**2**) above 400 nm are essentially of metal centered CT type [Fig.(II–10)] and their intensities grow with the progress of the oxygen atom transfer reaction with DMSO [8(a,b)]. The reaction of (**2**) with DMSO was followed at 401 nm and at four different temperatures in the range 300 – 325 K range. Additional time-dependent spectral studies indicated that (**1**) did not react with DMSO. The reaction (equation 1) is initiated through inner sphere electron transfer [e.g., concomitant with breaking of one of the bridges of the $(Mo^{V}_2O_4)^{2+}$ core], followed by relatively slow oxygen atom transfer reaction from the substrate, DMSO[19].

Table (II – 4): Kinetic data for DMSO reduction by (**2**) through oxygen atom transfer:

T (K)	k_{obs} x 10^3 (s^{-1})	$\Delta H^{\#}$ [a] (KJ mol^{-1})	$\Delta S^{\#}$ [a] (J mol^{-1} deg^{-1})	$\Delta G^{\#}$ [b] (KJ mol^{-1})
300	1.4			
309	1.9	25.5	– 206.3	
318	2.7			91.2
325	3.4			

[a] Values obtained from the Eyring plot; [b] values obtained from $\Delta G^{\#} = \Delta H^{\#} - T\Delta S^{\#}$ at 318 K.

$$(Mo^{V}_2O_4)^{2+} + DMSO \rightarrow (Mo^{VI}_2O_5)^{2+} + DMS \text{ ----- } (1)$$

The IR spectrum of the isolated oxidation product (Equation 1) shows two strong, broad bands at 936 and 902 cm^{-1} and a weaker band at 833 cm^{-1}, which can be correlated with the presence of $(Mo^{VI}_2O_5)^{2+}$ core in this case.

Kinetic data for DMSO reduction [Fig.(II–10)] by (**2**) are summarized in Table (II–4). The large negative activation entropy ($\Delta S^{\#}$) is consistent with an associative reaction mechanism. Rate constants for molybdenum centered oxygen atom transfer reactions determined by different authors on a variety of analogue reaction systems, are in line with the present data [8(a,b)]. To establish reaction stoichiometry, the reaction of (**2**) (0.3 mmol dm^{-3}) with DMSO was followed for 70 h (333 K, darkness) under continuous flow of N_2 and the emergin gas was passed into an aqueous solution of $HgCl_2$; the resulting precipitate of the known compound $(HgCl_2)_3(DMS)_2$ was estimated [8(d)]. Ca. 0.9 mol of DMS (b.p. 309 – 310 K) was recovered per mol of (**2**) added, according to equation (1) below.

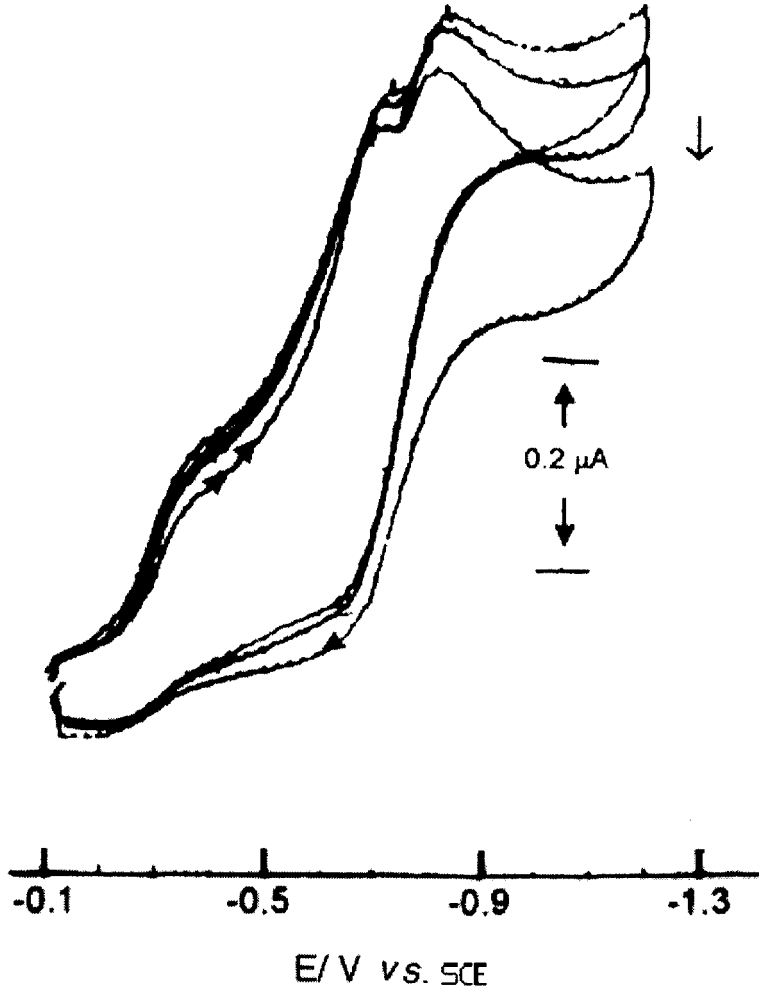

Fig.(II–11): CV scans during the progress of the reaction between (**2**) [$0.8x10^{-3}$ (M)] and DMSO. Data were recorded at 5 min. intervals using a Pt working electrode, Bu_4NClO_4 [0.1 (M)], scan rate 15 mVs^{-1}.

Reactions of $(Mo^{V}_{2}O_{4})^{2+}$ species involving breaking of one or both of the bridges, even conversion to mononuclear molybdenum (V) complexes could be achieved through careful choice of reagents / ligands [19]. Progress of the reaction between (**2**) and DMSO can also be monitored using cyclic voltammetry (CV) [Fig.(II–11)] indicating a gradual fall in concentration of the electro-active species. The cathodic reduction peak (E_{pc}) at – 0.84V and the two shoulders at – 0.74 and – 0.42V reflect reduction of the two molybdenum atoms [$Mo^{V} \rightarrow Mo^{IV}$], associated with rearrangement.

Conclusion

In concluding this discussion it can be said that the synthetic compound (**2**) bears functional resemblance to an appreciable extent to the oxomolybdoenzymes (particularly DMSO reductase here). The pterin ligand (**1**) here acts as a reducing agent and has reduced the Mo^{VI} starting material to Mo^{V} complex (**2**), which has been characterized through all possible physico-chemical means. This molybdenum – pterin complex undergoes oxygen atom transfer reaction with a typical enzyme substrate, DMSO and the kinetic parameters [Table (II–4)] of this reaction are at par with the available literature on this line [8(a,b)]. So. this new synthetic molybdenum – pterin compound (**2**) can be considered as a functional model to the DMSO reductase, an oxomolybdoenzyme.

CHAPTER II

SECTION – II

Synthesis and characterization of a molybdenum complex with sulphur and pterin ligands exhibiting saturation kinetics with pyridine N – oxide.

Abstract

Redox reaction between 6 – acetonyl-isoxanthopterin [$H_2(pte_1)$] and [$Mo^{VI}O_2(ssp)$] [ssp = anion of 2 – (salicylideneamino) benzenethiol] in CH_3OH – C_2H_5OH medium produces a new mixed ligand compound [$Mo^{IV}(ssp)(Hpte_1)(OCH_3)$]. It has been characterized by elemental analysis, Λ_M, ESIMS, UV–VIS, IR, ^1H NMR (1D & 2D), CHEM3D, fluorescence & CV data. Kinetics of formation of this compound as well as that of its reaction with pyridine N–oxide (PyN→O) have been followed spectrophotometrically. Both the reactions follow substrate saturation kinetics and involve metal centered oxygen atom transfer (OAT) process. Large negative values of entropy of activation ($\Delta S^{\#}$ = – 200.3 J mol^{-1} deg^{-1}) indicate the operation of associative mechanism.

Introduction

Recent X – ray structural characterization of several oxomolybdoenzymes reveal that a special pyranopterin [molybdopterin, Scheme (I – 1)] is coordinated to the molybdenum atom through a dithiolene group[1]. It has been proposed that the Mo(O) (molybdopterin) moiety is the Metal – centered Functional Unit (McFU) for such enzymes and variations in properties of the metal centre occur with the binding of other ligands, e.g., a terminal oxo or sulphido group, OH and / or H_2O group(s), a second pterin, and /or a serine, a cysteine or selenocysteine group from the polypeptide backbone of the pterin [1, 2]. Such enzymes catalyse formal hydroxylation (equation 1) and neat OAT reaction (equation 2), to and from a variety of biologically important substrates and the oxygen atom is ultimately derived from water [1].

$$RH + H_2O = ROH + 2H^+ + 2e^- \quad \text{----} \quad (1)$$

$$X + H_2O = XO + 2H^+ + 2e^- \quad \text{----} \quad (2)$$

Alternatively, (1) and (2) may be regarded as Coupled Electron Proton Transfer (CEPT) reactions. Intimate catalytic mechanisms proposed in (1) and (2) involve the coordination of water to the molybdenum atom to give Mo – OH_2, Mo – OH or Mo = O species which cycle between Mo(VI) and Mo(IV) oxidation states[1(a)]. The resolution of the X- ray crystal structures is insufficient for unambiguously resolving oxo, hydroxo and water ligands from one another, which leads to uncertainty in the oxidation state of the metal. Other limitations include uncertainty about the state of oxidation at the pyrazine ring carbon atoms or at the side-chain sulphur – bearing carbon atoms. Hence, the need for complementing the protein crystallographic results with spectroscopic data about the metal centers of these enzymes. In this context, the role of synthetic molybdenum – pterin compounds is vital for recording bench – mark data; development of such coordination Chemistry will also enable accomplishment of chemical and electrochemical studies that are relevant and complementary for the study of the functional aspects of the enzyme catalytic centers [1(b,c)]. Besides these, considerable challenge lies ahead to achieve a clear

description of how the nature of each of these metal centers changes during the operation of the enzyme's catalytic cycle as well as that of the corresponding molybdenum moiety. For explaining the DMSO reduction capability of a synthetic Mo^{IV} – pterin complex, Viscontini and co – workers [3(b), 4, 5(a)] proposed a model reaction cycle, which involves participation of the $NH_2(2)$ and NH(5) protons of the pterin ring [Scheme (II – 1)] associated with electronic redistribution in the later as well as in the oxo groups attached to the molybdenum centre.

In view of the above perspectives, the present work embodies the redox reaction of $[H_2(pte_1)]$ [6] [whose 7 – oxo group corresponds to the pyran ring oxygen atom of molybdopterin, Scheme (II – 1)] with a well – established dioxomolybdenum (VI) compound, $[Mo^{VI}O_2(ssp)]$, leading to the isolation of a new mixed ligand Mo^{IV} compound in the solid state. Its reactivity towards PyN→O, a typical enzyme substrate, has also been studied for corroborating the assignment of oxidation state of the metal centre [8].

Experimental

Materials: Reagent grade chemicals were used as received. Solvents were purified prior to use following the literature procedures [9]. Kinetic and electrochemical measurements were performed in spectroscopy grade DMF (SRL, Mumbai). 2–(salicylideneamino) benzenethiol (H_2ssp), $[Mo^{VI}O_2(ssp)]$, PyN→O and tetrabutyl ammonium perchlorate (TBAP) were obtained by published methods [7, 10, 11]. 6–acetonyl-isoxanthopterin $[H_2(pte_1)]$ was prepared by modifying its original method of synthesis in the light of subsequent developments (e.g., darkness, N_2 – atmosphere, pH 6.8) [6] and characterized through different physico-chemical methods including elemental analysis, ESIMS, and ^1H NMR spectra.

Method: Dinitrogen atmosphere was maintained by applying Schlenk technique in the synthesis and handling steps of the complex. Most of the physico-chemical methods were same as mentioned in Chapter II, Section I. Fig.(II–17) demonstrates the absorption spectral changes associated with the reaction of $[Mo^{VI}O_2(ssp)]$ with $H_2(pte_1)$ in DMF medium at 309 K. Kinetics of this reaction was followed at 400 nm and at four different temperatures in the range 299 – 324 K under pseudo – first – order conditions (maintaining 9 – 109 times excess of the pterin ligand). Observed rate constants (k_{obs}) were determined by least square method from the plots of $\log(A_t - A_\infty)$ vs. time, which were linear for at least three half – lives [8]. Fig.(II–18) shows the course of the change in absorption spectra (DMF, 298 K) over time resulting from the reaction of (**1**) with a typical enzyme substrate like, pyridine N-oxide (PyN→O) [8]. This reaction was monitored under similar conditions as above (at 400 nm, keeping about 13 – 130 fold excess of PyN→O).

Synthesis of the complex

$[Mo^{IV}(ssp)(Hpte_1)(OCH_3)]$ (1)

Complex (**1**) was synthesized by charging $H_2(pte_1).0.5H_2O$ (0.244 g, 1 mmol) in CH_3OH (100 ml) to a suspension of $[Mo^{VI}O_2(ssp)]$ (0.355 g, 1 mmol) in EtOH (50 ml), and stirred for 30 h at RT (301 K), in darkness under dinitrogen atmosphere. The resulting chocolate – brown compound was filtered under N_2 using glass- fritte, washed with purged solvents (CH_3OH, Et_2O) and dried in vacuo over silica-gel. Yield : 50 %. Solubility ca. 6.5 % in DMSO. Its purity was checked through TLC (Silica – gel GF_{254} ; UV–lamp) using diluted (with 50 times CH_3OH) DMSO solution (ca. 0.5 %) and benzene as eluant. R_f: 0.54. Found : C, 47.1 ; H, 3.2 ; N, 14.5 ; S, 5.2; Mo, 16.5 %. Calc. for $C_{23}H_{19}N_6O_5SMo$: C, 47.0 ; H, 3.2 ; N, 14.3 ; S, 5.4; Mo, 16.4 %. UV–VIS absorption bands [DMF, $\lambda_{max}^{nm}(\log\epsilon)$]: 285 (4.23); 320 (4.16); 338 sh (4.13); 398 (3.85); 424 sh (3.70); 458 sh (3.46). The compound is found to be diamagnetic in nature.

Results and Discussion

As stated above, ESIMS has proved to be a valuable method to establish molecular formula and assigning the fragmentation or fragment association peaks formed during ESIMS life- time [12]. This technique can be applied to characterize wide variety of compounds including inorganic and coordination compounds [110, 121]. Similar to different types of mass spectrometry, the assignment of molecular formula (or any definite fragment originating from it) is confirmed by the experimental value of m/z (most abundant isotopic mass) as well as matching between the experimental and calculated (simulated) isotopic distribution profile [14, 85, 107, 117, 118]. As far as organic compounds containing O, F, P and I are concerned, the relative intensities of M, M+1 and M+2 isotope peaks are of great value in recognizing the molecular ion (M^+) peak or any well – defined fragment confirming it [85]. An M–1 peak is common and occasionally an M–2 peak (loss of H_2) or even a rare M–3 peak (from alcohols) is reasonable [85]. Absence of molecular ion (or an extremely weak M^+ peak) is characteristic of highly branched molecule [85, 107]. For (**1**), the peak at m/z = 525.0 (relative abundance 100 %), associated with the characteristic distribution of molybdenum isotopes (seven) for mononuclear species, corresponds to the fragment [M–2CH_3O (1 CH_3O from the coordination sphere and another from 6 – acetonyl substituent)]$^+$, where 'M' is the molecular formula of (**1**) (F.W. = 588)[7(a), 14, 15]. The molecular ion peak appeared at m/z = 584.8 [M – 3H]$^+$. A couple of peaks arising out of deprotonation of the (**1**), isotopic distribution of Mo atom in (**1**) are centered around the molecular ion peak. These peaks are simulated by IPC [46] [Fig.(II–12)] and found to be in good matching between the calculation result and that of the experimentally found one. From the above discussion it can be inferred that (**1**) is a mononuclear species [Fig.(II–16)], comparable to a related characterized complex through X- ray crystallography [3(a)].

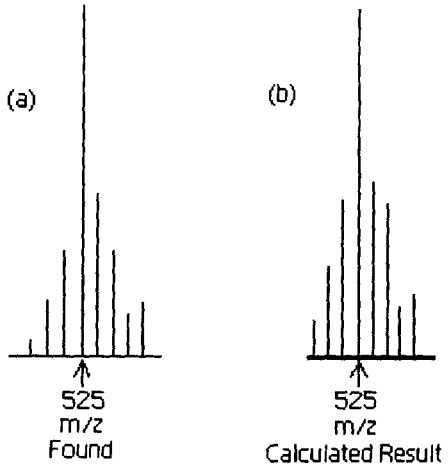

Fig.(II–12): (a) ESIMS data of (**1**) at m/z (= 525) region corresponding to $[M - 2CH_3O]^+$; (b) the calculated isotope pattern [46]. Formula: $C_{21}H_{11}N_6O_3MoS$.

The Λ_M value (20 ohm $^{-1}$cm ^{2} mol $^{-1}$, 303 K, DMF) is consistent with its non-electrolytic nature [13].

A comparative study of the IR spectra (nujol, cm $^{-1}$) of (**1**) and that of the ligand, $H_2(pte_I)$ throws light on the nature of donor sites in the ligand residue ($Hpte_I^-$) as well on the Mo – centered oxygen atom transfer occurring during its formation. IR absorptions typical of terminal ν(Mo = O) at 930 cm $^{-1}$ and bridging ν(Mo = O → Mo) at 780 cm $^{-1}$ of $[Mo^{VI}O_2(ssp)]$ are absent in the IR spectrum of (**1**)[7(b), 17], indicating the removal of such oxygen entities through reaction with the redox "non- innocent" pterin ligand. The residual IR band at 780 can be correlated with the IR absorption of the (ssp^{-2}) residue, as verified through recording of IR spectrum of H_2ssp[7(a)]. The intense IR bands in the region 1700 – 1600 cm^{-1} of the free ligand are modified significantly on coordination to the molybdenum atom in (**1**), reflecting enolisation of the 4 – oxo group followed by coordination of the ($Hpte_I^-$) residue involving the O(4), N(5) atoms, where the Mo – N(5) bond plays a pivotal role [3(b), 5, 19]. The ν(C = O) modes of the 2′ and 7 – oxo groups appear together at 1625 cm $^{-1}$ as a strong broad band in (**1**) ; the ν(CH = N) mode of the azomethine group (observed at 1598 cm $^{-1}$) in (**1**) and the ν(C = C), ν(C = N) vibrations of the pterin ring lie hidden under this band [5]. Now, considering the tridentate ONS donating (ssp^{2-}) residue and the (CH_3O) group, a coordination number of six can be inferred for the Mo^{IV} atom in (**1**) [Fig.(II–16)][7(a), 18(a)].

Of the three chemically relevant oxidation states of molybdenum (e.g., Mo^{IV}, Mo^{V} and Mo^{VI}), during catalysis in oxomolybdoenzymes, the Mo^{IV} (d^2) state is consistently diamagnetic [26]. Almost all the synthetic molybdenum pterin complexes reported so far are diamagnetic; their diamagnetic behaviour is explained by invoking a strong antiferromagnetic coupling between the d – electrons of the Mo – atom and the delocalized electron system of the redox "non-innocent" pterin ligand [20(a,d)]. This unique nature of pterin ligand is responsible for the observed diamagnetism of (**1**) and its high resolution ^{1}H NMR data [Fig.s(II-13) to (II-15)].

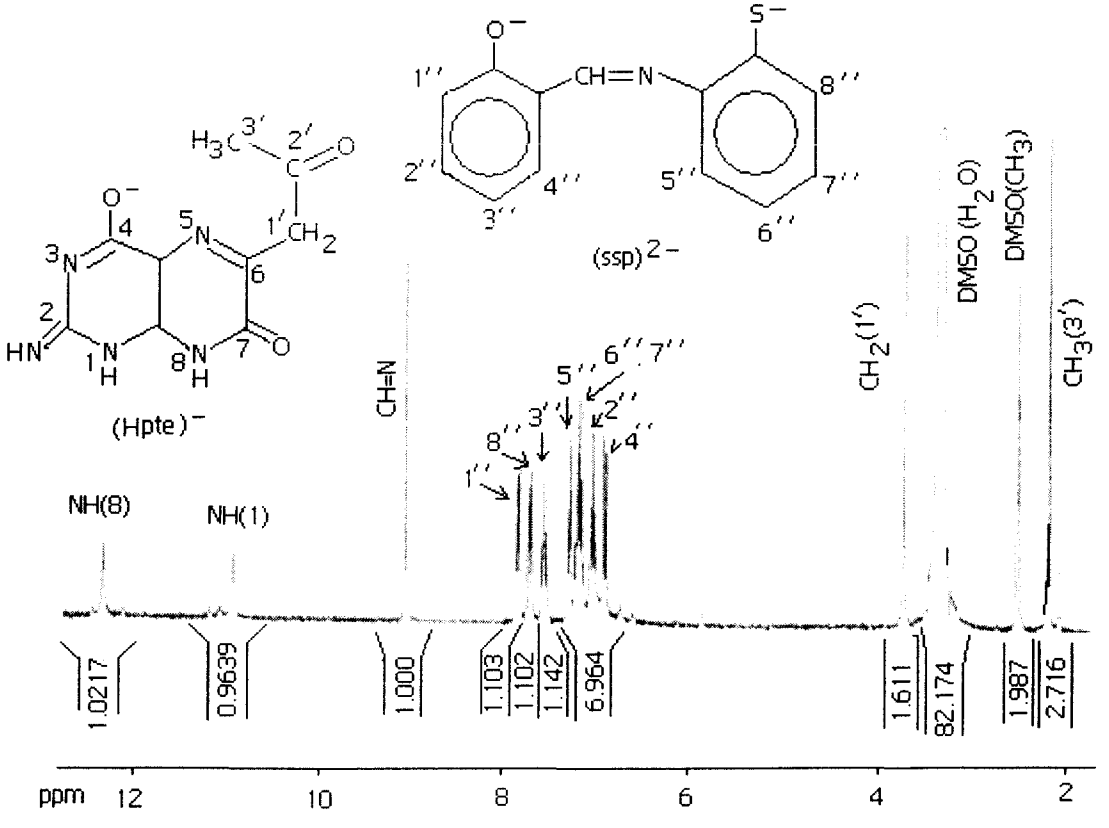

Fig.(II –13): 300 MHz ^{1}H NMR spectrum in DMSO – d_6 (δ, ppm vs. TMS) of **(1).**

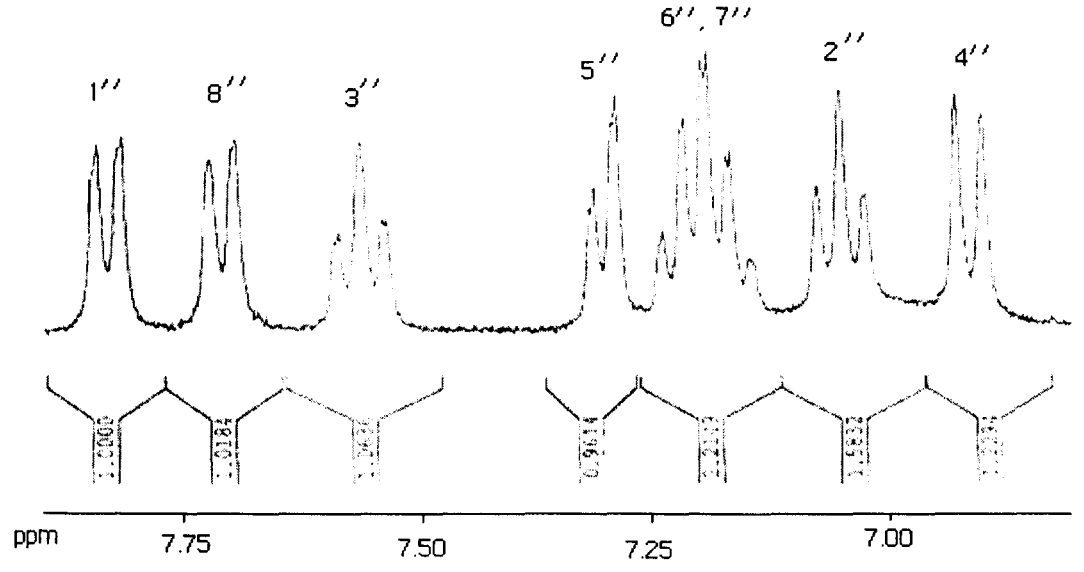

Fig.(II–14): 300 MHz ^{1}H NMR spectrum (expanded) in DMSO – d_6 (δ, ppm vs. TMS) of **(1)**.

^{1}H NMR data of **(1)** have been assigned on the basis of the expanded spectrum (δ, 8.0 – 6.5) [Fig.(II–14)], the corresponding ^{1}H – ^{1}H COSY data [Fig.(II–15)], protonic integration values and ^{1}H NMR data of $H_2(pte_1)$. A tautomeric form of ($Hpte_1^-$) residue involving protons of the N(1) and N(2) atoms [90] [Scheme (II–1)], is consistent with these data. $CH_3(3')$, $CH_2(1')$, NH(1) and NH(8) signals of the ($Hpte_1^-$) residue appear as singlets at δ, 2.18; δ, 3.74; δ, 10.96 and δ, 12.34 respectively [16]. The characteristic azomethine (CH = N) signal at δ, 9.06 (singlet) of the (ssp^{2-}) residue is consistent with the observed data for closely related chelated ligand residues (ONO/ONS donors) in well–characterized coordination compounds of molybdenum [7(a), 17]. The protonic integration values of these signals [e.g., NH(8) and CH = N – protons] indicate a 1 : 1 ratio of (ssp^{2-}) : ($Hpte_1^-$) in **(1)**. The proton signal of the (CH_3O) residue is covered by the residual H_2O signal (of DMSO – d_6) at δ, 3.55. Importance of the molybdenum – methoxide interaction has been pointed out by several authors and established through X – ray crystal structure determination in one case[18]. For $H_2(pte_1)$, the $CH_3(3')$, and $CH_2(1')$ proton signals (s)

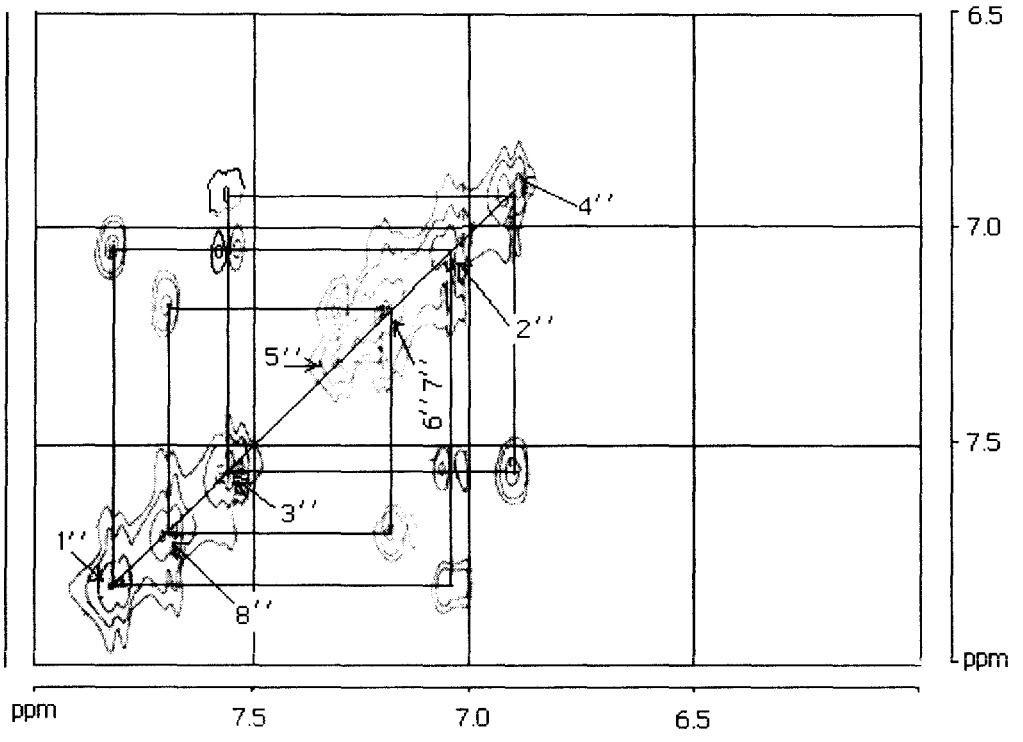

Fig.(II – 15): 300 MHz $^{1}H - {}^{1}H$ COSY data of (**1**) in DMSO – d_6.

appear at δ, 2.18 and δ, 3.74 respectively [vide Table(II-1)]; in (**1**) δ values of these proton signals for the ($Hpte_1^-$) residue remain essentially unchanged, thereby indicating that the O(2′) atom [Scheme (II–1)] remains uncoordinated. Besides this, ^{1}H NMR data of (**1**) also indicate that the $NH_2(2)$ group exists here as shown in Scheme (II–1), with its two protons appearing essentially as a broad signal at δ, 7.0. However, during the complex formation redox reaction a tautomeric change takes place and the NH(1) signal appears at δ, 10.96 in (**1**) ; this supports participation of the pterin ring during oxygen atom transfer reaction occurring at the molybdenum centre [3(b)]. The = NH(2) proton signal of (**1**) lies hidden under proton signal of the (ssp^{2-}) residue, as evident from protonic integration data of the expanded spectrum.

From consideration of elemental analysis and ESIMS data (experimental and simulated) as well as other physicochemical data, the chemical compositions of the new compound was established. Then its possible schematic structure was optimized by molecular mechanics calculation (MM2), giving the lowest steric energy (= 13.2 Kcal mol $^{-1}$) CHEM3D model [Fig.(II–16)], thereby throwing light on both stability and geometry of this compound [87]. The molecular modeling force fields in use for molecular systems can be interpreted in terms of the four key contributions, e.g., bond stretching, angle bending, torsional terms and non-bonded interactions [86] ; apart from the lowest steric energy of the molecule, two basic parameters were evaluated, e.g., bond distances (Å) and bond angles (deg.), the most relevant of which are shown in Table(II–5) together with the literature data obtained through X-ray structural studies on molybdenum complexes with different pterin ligands and relevant compounds [3, 5, 20(a-c), 27, 29, 114 - 116]; this is in conformity with the recent trends of structure elucidation using optimized computational models[48, 86, 108, 179] .

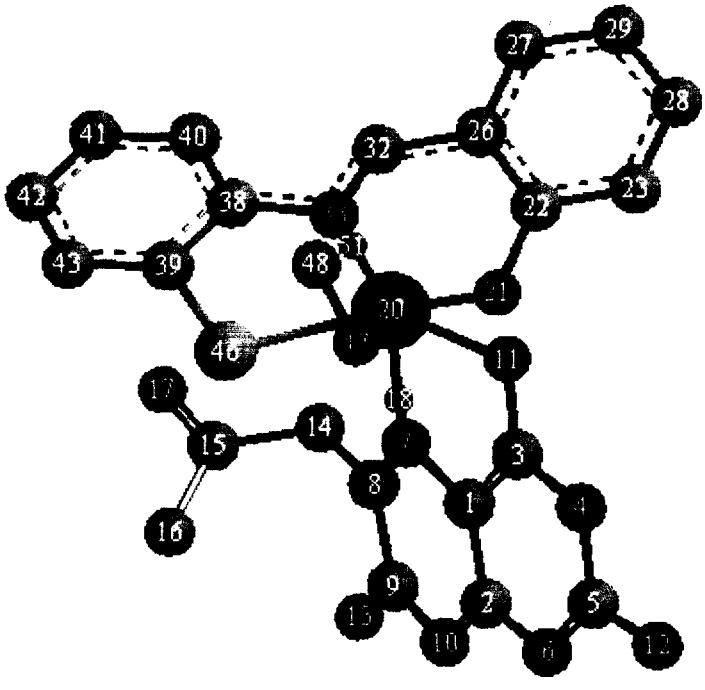

Fig.(II–16): The optimized geometry (CHEM3D model obtained through MM2 calculations) of (1) with a steric energy of 13.2 Kcal mol^{-1}. Its numbering system is set by the software used[87] and is different from that in Scheme (II – 1).

Table (II–5): Comparison of selected computed bond lengths(Å) and bond angles (deg.) involving Mo – atom in (**1**) from the optimized geometry [Fig.(II–16), MM2 calculations] with the available literature data (in parenthesis) from X-ray structural studies*

Atoms	Bond Distances(Å)+	Atoms	Bond Distances(Å)+
N(33)-Mo(20)	2.12(2.16)[108]	S(46)-Mo(20)	2.37(2.37)[109, 110]
N(7)-Mo(20)	2.10(2.02)[3(c)]	Mo(20)-O(21)	1.98(1.70)[109]
O(47)-Mo(20)	1.98(2.32)[109]	O(11)-Mo(20)	1.10(2.23)[3(c)]

Angle Atoms	Bond Angle(deg.)+	Angle Atoms	Bond Angle(deg.)+
N(33)-Mo(20)-S(46)	76.7(77.5)[109]	N(7)-Mo(20)-O(11)	82.8(74.1)[3(c)]
O(21)-Mo(20)-O(11)	74.2(78.1)[109]	Mo(20)-N(7)-C(1)	118.2(119.3)[3(c)]
C(3)-O(11)-Mo(20)	112.9(112.1)[3(c)]	O(47)-Mo(20)-N(7)	103.2(103.3)[109]
N(33)-Mo(20)-O(21)	78.1(82.9)[109]	Mo(20)-N(33)-C(38)	127.0
N(33)-Mo(20)-N(7)	106.9	N(7)-Mo(20)-O(21)	74.8
N(7)-Mo(20)-S(46)	80.6	S(46)-Mo(20)-O(11)	136.2
S(46)-Mo(20)-O(21)	137.5	S(46)-Mo(20)-O(11)	136.2

+ Here O(11), N(7) and O(17) correspond to O(4), N(5) and O(2′) donor atoms respectively, of the pterin ring as per Scheme (II – 1), while N(12) and N(6) correspond to the 2-substituent N and N(1) respectively.

* X-ray structural data have been collected from references mentioned as superscript on the data within parenthesis.

Concentrating on the chelating aspect of the pterin ligand towards molybdenum, the Mo-N(5) bond plays a pivotal role here [Scheme (II – 1) indicates the O(4), N(5) etc, numbering system] and this bond distance shows a fair agreement between the computed and experimental data [3, 5, 20(a-c), 27, 29, 114 – 116]. The calculated Mo-O(4) bond distance is slightly shorter than the available X – ray structural data, but this value is close to the Mo – O_b bond distance (1.88 – 1.97 Å) of Mo – O_b – Mo bridges (of binuclear complex) and is much longer than the terminal Mo=O_t bond distance (1.66 – 1.67 Å).

Fig.(II–16) represents the most stable CHEM3D form of (**1**). In this form, the pterin ligand acts as an uni-negative ($Hpte_l^-$) O(4), N(5) donor; where O(4) made a covalent bond and N(5) a coordinate bond with the Mo^{IV} atom. The (ssp^{2-}) residue, which acts as a bi- negative ONS donor, coordinates to the metal atom through Mo – O & Mo – S covalent bond formation and one Mo – N coordinate bond formation (through the lone pair of N). One CH_3O group is also coordinated to the Mo^{IV} atom. The bond between the N(5) and Mo^{IV} forms the apex position of the pentagonal pyramidal geometry and other five bonds form the plane of this geometry in the molecule. Other possible structures of the complex originated by changing the positions of π – bonds in the pterin part also have almost similar stability. In all the cases the Mo – centre retained its pentagonal pyramidal geometry, but the variation is in the position of π – bonds. It is clear from these structures that a double bond at C(6) – C(1′) position brings some instability to the molecule. The CHEM3D representations containing aromatic pterin ligand residue were less stable than the non – aromatic one.

Table (II – 6): Comparison of selected optimized bond lengths (Å) and bond angles (deg.) in the free ligand, $H_2(pte_l)$ and its molybdenum complex (**1**).

Atoms	Bond Distances(Å)$^+$	Atoms	Bond Distances(Å)$^+$
C(1)-N(7)	1.41 [1.44]	C(1)-C(3)	1.48 [1.36]
C(3)-O(11)	1.22 [1.37]	C(1)-C(2)	1.37 [1.45]
C(9)-O(13)	1.22 [1.23]	C(3)-N(4)	1.37 [1.40]
C(2)-N(6)	1.40 [1.39]	C(9)-N(10)	1.36 [1.37]
C(15)-C(16)	1.51 [1.51]	C(5)-N(12)	1.37 [1.38]
C(2)-N(10)	1.35 [1.32]	C(5)-N(6)	1.31 [1.33]
N(7)-C(8)	1.28 [1.30]	C(14)-C(15)	1.51 [1.51]
C(8)-C(9)	1.49 [1.50]	N(4)-C(5)	1.35 [1.38]
C(15)-O(17)	1.21 [1.21]	C(8)-C(14)	1.50 [1.51]

Angle Atoms	Bond Angle(deg.)[+]	Angle Atoms	Bond Angle(deg.)[+]
N(6)-C(5)-N(4)	120.87 [122.84]	C(1)-N(7)-C(8)	118.67 [110.91]
C(3)-N(4)-C(5)	124.83 [122.34]	C(1)-C(3)-N(4)	114.84 [115.11]
C(8)-C(9)-N(10)	114.90 [121.42]	N(6)-C(2)-C(1)	121.60 [119.16]
N(7)-C(8)-C(9)	122.95 [123.34]	N(10)-C(2)-C(1)	119.78 [117.95]
C(2)-N(10)-C(9)	122.73 [118.50]	N(7)-C(1)-C(2)	120.97 [127.01]
C(2)-N(6)-C(5)	119.69 [117.92]	C(3)-C(1)-C(2)	118.17 [122.45]

[+] Free ligand data are mentioned outside third bracket and the data derived from its molybdenum complex, (**1**), are mentioned within third bracket.

Tables (II–6) shows the bond lengths and bond angles of the free ligand and that of the pterin ligand residue in the complex (**1**). Comparing these two sets of data it is clear that both bond lengths and bond angles of the pterin rings have undergone a visible change in it's complex suggesting definite complexation of the pterin ligand with molybdenum metal. The above discussion on the geometrical aspect of optimized computational model (MM2) of a new complex compound, having agreement with available X-ray structural data (e.g., bond length, bond angle and overall geometry) verifies the applicability of such an approach to molybdenum – pterin systems and provides the frame work for discussion on their spectroscopic, reactivity and other relevant aspects [88(a), 108, 120].

UV – VIS absorption spectrum of the complex contains all the characteristic bands of pterin ligand including a peak at 320 nm characteristic of the (ssp^{2-}) residue. Comparison of the UV – VIS spectral data of pterin ligand and that of (**1**) indicates that there are considerable increase in intensity (logε – value) of the ligand bands (essentially $\pi \rightarrow \pi^*$ type) through complex formation. This is in conformity with the – $NH_2(2)$ lone pair electrons' flow towards the metal atom through the pterin ring during complex formation.

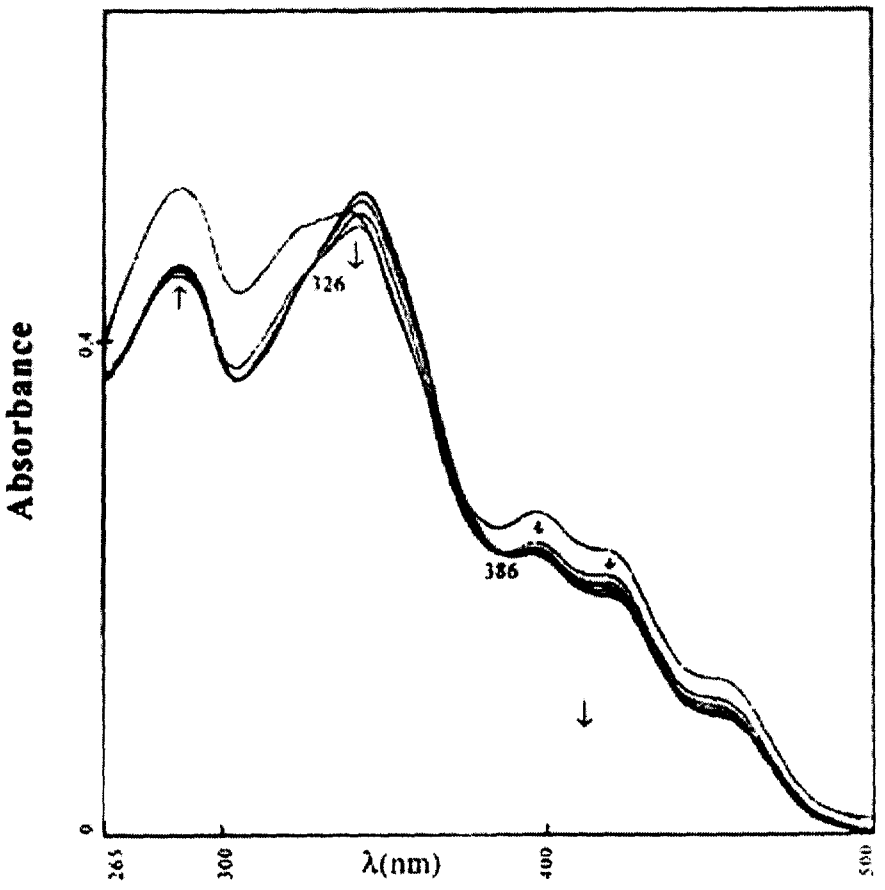

Fig.(II–17): Absorption spectral changes recorded every 8 min. during the reaction of $[Mo^{VI}O_2(ssp)]$ [3.0 x 10^{-6} (M)] and H_2pte_1 [7.0 x 10^{-5} (M)] in DMF solution at 309 K.

Reactivity of (**1**) towards PyN→O indicates that the molybdenum atom here exists in a lower oxidation state, e.g., Mo^{IV}. The relevant oxidation product was isolated by reacting (**1**) (328 K, darkness, 5 h, DMF) with PyN→O (in 1 : 3 molar ratio), followed by evaporation in a rotary evaporator, treatment of the residue with CH_3OH, filtration and washing with ether; elemental analysis indicated the composition $[(Mo^{VI}_2O_5)(Hssp)(Hpte_1)]$. 0.5DMF. The ν(Mo = O) and ν(Mo – O – Mo) modes characteristic of the $(Mo^{VI}_2O_5)^{2+}$ core are observed at 925, 888 and 825 cm^{-1} respectively [20]. Most likely the initial product [e.g., possessing the $(Mo^{VI}O)^{4+}$ core] of PyN→O oxidation undergoes hydrolysis with the moisture present in the solvents and μ – oxo dimerization reaction, giving ultimately the $(Mo^{VI}_2O_5)^{2+}$ core [Equations: 5(a) – 5(c), below] [19, 20(c,d)].

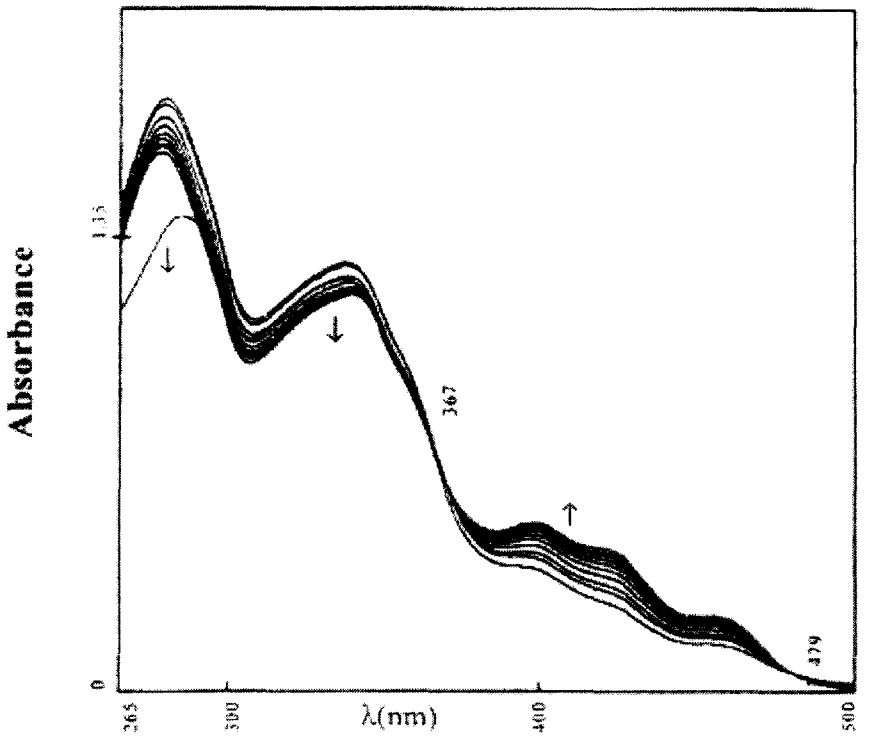

Fig.(II–18): Absorption spectral changes recorded every 3 min. during the reaction of (**1**) [3.4 x10^{-4}(M)] and PyN→O [2.5 x 10^{-2}(M)] in DMF solution at 298 K.

Fig.s (II–17) & (II–18) represent the spectrophotometric monitoring of the reaction of [$Mo^{VI}O_2$(ssp)] with [$H_2(pte_1)$] and that of (**1**) with PyN→O respectively [21(a,b)]. In the first figure isosbestic points are observed at 326 and 386 nm, while two isosbestic points can be identified at 367 and 479 nm in the second figure. Both the reaction systems exhibit substrate saturation kinetics at sufficiently high substrate concentration [Fig.s(II–19) & (II–20)] [21]. Under these conditions, the reactions are first order in [$Mo^{VI}O_2$(ssp)] and (**1**) respectively, as shown by linear plots of log ($A_t - A_\infty$) vs. time, from which the observed rate constants were obtained [8(a,c), 17, 23].

The reaction [Scheme (II–3)] leading to the formation of (**1**), i.e., the mixed ligand Mo^{IV} compound, is initiated through reversible substrate [S], i.e., [$H_2(pte_1)$] binding followed by oxo transfer (along with coupled electron proton transfer) with rate constant k_2. During isolation of the product on preparative scale in presence of methanol, further reactions occur with loss of both the oxo groups of [$Mo^{VI}O_2$(ssp)], giving (**1**) as the ultimate product. Loss of oxo ligands, during complex formation involving $(Mo^{VI}O_2)^{2+}$ starting materials, is rare with conventional ligands unless an oxo abstractor

like PPh_3 / Ph_2MeP is present [7(a,c), 17, 23(a)]. In terms of Scheme (II–3), below, the k_{obs} can be represented as follows [22] :

$$k_{obs} = k_2[S]/(K_M + [S]) \quad \text{---- (3)}$$

Where, $K_M = (k_2 + k_{-1})/k_1$,

Or,

$$1/k_{obs} = 1/k_2 + K_M/k_2[S] \quad \text{---- (4)}$$

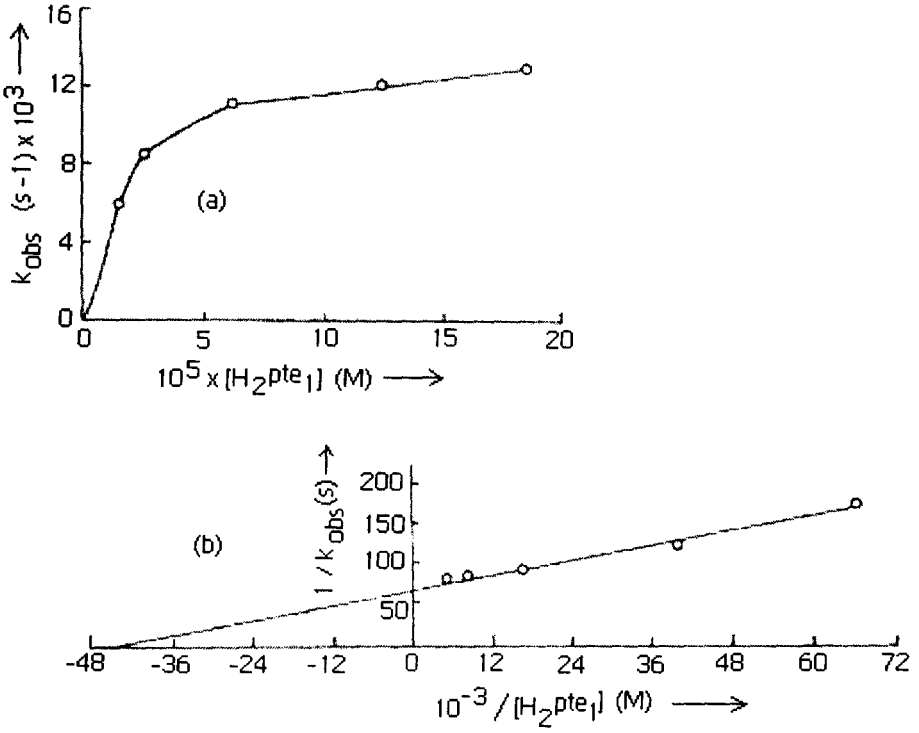

Fig.(II–19): (a)Dependence of the rate of reaction of [$Mo^{VI}O_2$(ssp)] [1.7 x 10^{-6} (M)] with $H_2(pte_1)$ in DMF at 299 K;(b) the corresponding double reciprocal plot.

A plot of the k_{obs} vs. [$H_2(pte_1)$] in shown in Fig.(II–19a). The plot of 1/ k_{obs} vs. 1/[H_2 (pte_1)] should give a straight line with 1/ k_2 as the intercept and K_M/k_2 as the slop. The x – axis intercept equals 1/ K_M. From the double reciprocal plot of 1/ k_{obs} vs. 1/[$H_2(pte_1)$] [Fig.(II–19b)], k_2 and K_M were calculated as 1.5x10^{-2} s^{-1} and 2.2 x 10^{-5} mol dm^{-3} respectively at 299 K. The value of k_2 is comparable in magnitude to those of molybdenum mediated oxygen atom transfer reactions obtained using a wide variety of model compounds and substrates [8, 17, 23].

$$[Mo^{VI}O_2(ssp)] + H_2(pte_1) \underset{k_{-1}}{\overset{k_1}{\rightleftharpoons}} \{Mo^{VI}O_2(ssp)(H_2(pte_1))\} \xrightarrow{k_2} Mo^{IV} \text{ mixed ligand compound (1)} + \text{Other products (e.g., } H_2O)$$

[Scheme (II – 3]

$$\text{Compound (1)} + PyN{\rightarrow}O \underset{k_{-1}}{\overset{k_1}{\rightleftharpoons}} \{\text{Compound(1)}(PyN{\rightarrow}O)\} \xrightarrow{k_2} Mo^{VI} \text{ mixed ligand compound} + PyN$$

[Scheme (II – 4)]

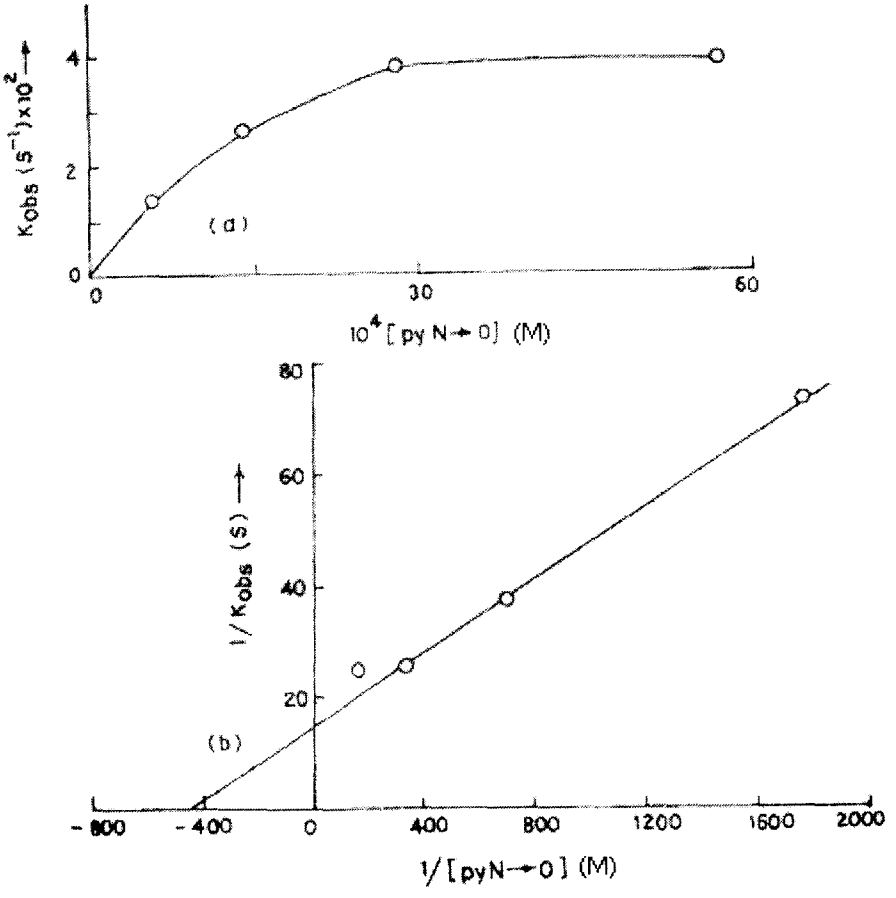

Fig.(II–20): (a)Dependence of the rate of reaction of (**1**)[4.4 x 10^{-5} (M)] with PyN→O in DMF at 299 K; (b) the corresponding double reciprocal plot.

Activation parameters [$\Delta H^{\#}$ = 11.3 KJ mol $^{-1}$; $\Delta S^{\#}$ = - 200.8 JK $^{-1}$ mol $^{-1}$] were obtained from the Eyring plot [ln(k / T) vs. 1/T] using pseudo – first order rate constant data determined [keeping a 90 fold excess of $H_2(pte_1)$] at different temperatures. The negative activation entropy is consistent with the proposed associative mechanism [Scheme (II–3)] [24].

Scheme (II–4) represents the possible pathway of the reaction between (**1**) and PyN→O in DMF medium, which involves the reversible formation of an intermediate containing both the reactants, followed by its transformation to the products. Reaction stoichiometry was established by estimating the amount of pyridine released through the reaction (328 K, 50 h, N_2 atm., darkness) of a known weight of (**1**) with 10 equivalents of PyN→O; pyridine was estimated gravimetrically as the known compound $[Zn(C_5H_5N)_2](SCN)_2$ from the petroleum ether extract of the reaction medium [25]. About 2 moles of pyridine were recovered per mol of (**1**) added as per the following equations :

2 Compound (**1**) + 2 PyN→O ⟶ 2[$Mo^{VI}O$] $^{4+}$ complex + 2PyN ---- 5(a)

2[$Mo^{VI}O$] $^{4+}$ complex + 2PyN→O + H_2O ⟶ [$Mo^{VI}_2O_5$]$^{2+}$ complex + 2PyN + $2H^+$ ---- 5(b)

Overall reaction :

2 Compound (**1**) + 4 PyN→O + H_2O → [$Mo^{VI}_2O_5$]$^{2+}$ complex + 4 PyN + $2H^+$ ---- 5(c)

The plot of (k_{obs}) vs. [PyN→O] is shown in Fig.(II–20a). Assuming the validity of equations (3) and (4), above, in this case as well, the double reciprocal plot of $1/k_{obs}$ vs. $1/[PyN→O]$ [Fig.(II–20b)] was utilized for the calculation of $k_2 = 6.7x\ 10^{-2}\ s^{-1}$ and $K_M = 2.3 \times 10^{-3}$ mol dm^{-3} at 299 K. Variable temperature pseudo – first order rate constant data (determined using 80 fold excess of PyN→O) were used for calculating the activation parameters ($\Delta H^{\#}$ = 3.8 KJ mol^{-1}; $\Delta S^{\#}$ = - 200.3 JK $^{-1}$mol^{-1}) from the Eyring plot. The negative $\Delta S^{\#}$ value supports the formation of an intermediate as shown in Scheme (II– 4) above. The k_2 – value is in line with the existing rate constant data for oxo transfer reactions of various Mo^{IV} complexes with PyN→O and other similar substrates [8(c), 23(b)].

The voltammogram of (**1**) is characterized by single irreversible reduction peak [$Mo^{IV} \rightarrow Mo^{III}$] at – 0.82V (50 mV s^{-1}), is in conformity with the presence of only one Mo – atom in its formula. The pterin ligand itself undergoes reduction beyond – 1.8 V [12].

Conclusion

ESIMS data in conjunction with elemental analysis data and supported by IR and ^{1}H NMR spectral studies, verify the **formulations / chemical compositions** of the new complex (**1**). Molecular modeling studies [CHEM3D models obtained through MM2 calculations] provide with its optimized molecular geometry as well as bond length and bond angle data. The later type of parameters are in agreement with the published X-ray structural data on different molybdenum – pterin coordination compounds in related systems. This aspect verifies their **molecular structures**.

^{1}H NMR and IR spectral data point out that $H_2(pte_1)$ exhibits redox "non-innocent" behaviour during its reaction with [$Mo^{VI}O_2$(ssp)]; the loss of oxygen atoms of the latter [leading to the formation of (**1**)] is accompanied by a tautomeric change involving the NH_2(2) group and related electronic redistribution in the pterin ring. The process is characterized by substrate saturation kinetics and may be regarded as a coupled electron proton transfer reaction. On the other hand, the reaction between (**1**) and PyN→O is essentially an oxygen atom transfer process, conforming to substrate saturation kinetics as well and throwing light on the **oxidation state of the molybdenum atom** in (**1**). The final product in 5(c) reflects the role of hydrolysis and μ – oxo dimerization reaction. The reductive half reaction of xanthine oxidase with sub - stoichiometric amounts of xanthine exhibits substrate saturation kinetics with faster k_2 values [21(c)].

Finally, the role of the solvent used for the preparative purpose here (e.g., CH_3OH) is to be assessed vis-à-vis that of H_2O in the catalytic cycle of oxo molybdoenzymes. Loss of an oxo group from the Mo^{VI} species during enzyme turnover is made up by the H_2O molecule giving $Mo–OH_2$ and undergoes facile deprotonation to Mo–OH or Mo = O species accompanied by changes in the oxidation state of the metal centre [1(a), 26]. During formation of (**1**), loss of oxo groups from $[Mo^{VI}O_2(ssp)]$ is made up partly by the pterin ligand residue ($Hpte_l^-$) [20(a)] and partly by the solvent molecule (CH_3OH); through the formation of CH_3O^- group [18] and charge balance is chieved.
